Parameter Estimation of the Hamiltonian of the Nitrogen-Vacancy Center in Diamond

Parameterschatting van de Hamiltoniaan van de Nitrogen-Vacancy Center in Diamant

Rebecca Gharibaan

To obtain the degrees of Bachelor of Science in Applied Mathematics and Applied Physics
at the Delft University of Technology
to be defended publicly on Tuesday July 16th, 2019 at 15:30

Faculty of Electrical Engineering, Mathematics and Computer Science and Faculty of Applied Sciences
TU Delft
The Netherlands
August 13, 2019

Parameter Estimation of the Hamiltonian of the Nitrogen-Vacancy Center in Diamond

Parameterschatting van de Hamiltoniaan van de Nitrogen-Vacancy Center in Diamant

Rebecca Gharibaan

Student Number:	4281012
Project Duration:	October, 2018 - July, 2019
Committee:	T.H. Taminiau (supervisor)
	J. Dubbeldam (supervisor)
	M. Blaauboer
	M. B. Van Gijzen

Special thanks to my supervisor J. Randall for helping me with this project.

Contents

1 Introduction

A new and exciting quantum era is upon us, as technologies such as quantum internet and quantum computing are rapidly developing. With quantum internet it will be possible to securely transfer information, and combined with quantum computing, challenges such as breaking encryptions on classical computers can be overcome. However, to implement such a quantum internet, we need reliable quantum bits that minimize information loss [1]. The Nitrogen-Vacancy (NV) center in diamond shows a promising future in solving this problem. In order to gain better understanding of the NV center, the parameters in its Hamiltonian will have to be better understood quantitatively. In this report, it will be analysed how to obtain the parameters using frequency measurements.

The Hamiltonian of the NV center contains unknown parameters, such as the zero-field splitting and the magnetic field. Knowing how the frequency measurements depend on the parameters will give greater understanding of the NV center. Including the nitrogen nuclear spin gives us the opportunity to find more parameters such as the quadrupole splitting. Analytically finding expressions for all of these parameters is very time consuming to do, and therefore the method of second order perturbation is used in this report to find approximations. With this method, estimations of the eigenvalue differences and parameters were found, including new estimations for the quadrupole splitting. As we don't exactly know whether the quadrupole splitting is positive or negative, there are two estimates found given by $\Delta_Q^+ = 4949.25(2)$ kHz and $\Delta_Q^- = -4949.11(1)$ kHz.

2 Method

Consider a diamond lattice. In practice, this lattice contains impurities as shown in figure 1. The Nitrogen-Vacancy (NV) center consists of an empty space in the lattice with a nitrogen atom next to it. The NV center can be considered a spin-1 ($S = 1$) particle and in this report it will be referred to as 'the electron', where the spin will be denoted as m_s. The electron is either in its ground state, $m_s = 0$ or in one of the (degenerate) excited states, $m_s = \pm 1$. The frequencies of the spin transitions $m_s = 0 \rightarrow \pm 1$ can be measured. By applying a magnetic field along the NV axis, we can lift the degeneracy of the excited states. Then we can measure different frequencies for spin transitions $m_s = 0 \rightarrow +1$ and $m_s = 0 \rightarrow -1$.

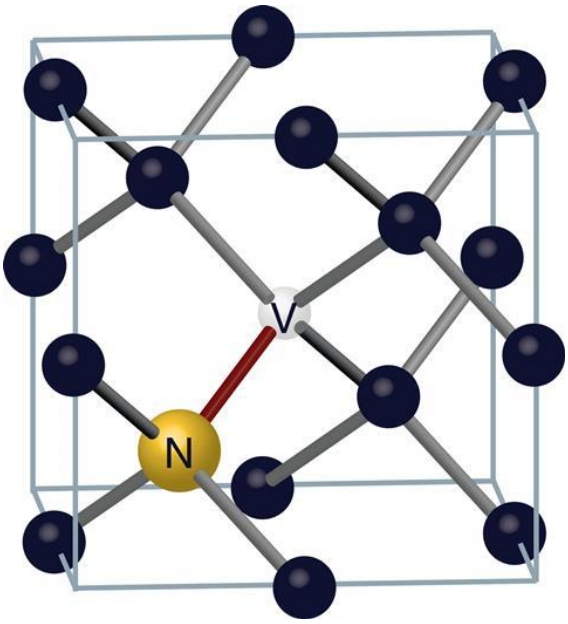

Figure 1: A diamond lattice with an NV center consisting of a nitrogen atom (yellow) and a vacancy (white). Figure from [8].

The eigenfrequencies of the NV center Hamiltonian depend on several factors. To sum up a few:

- The magnetic field alignment.
- The strain on the crystal influences the energy levels of the electron associated with their respective spin states.
- The nitrogen atom has a nuclear spin, which splits the energy levels of the electron.
- The ^{13}C atoms within the lattice have a nuclear spin which affect the electron's energy levels.

The effects of the first three influences will be explored in this report. From the Hamiltonian, these influences can be described in a quantitative way by finding its eigenvalue differences which correspond to the frequency differences in electron spin transitions, and further in this report also the nitrogen nuclear spin transitions. However, finding analytic expressions for these can get quite time consuming as more factors are taken into consideration. This will also make it more complex to extract the parameters from the Hamiltonian. To simplify this process, in practice we make approximations by neglecting terms. We can also solve this problem numerically.

Instead of attempting to find analytic expressions which is time consuming or find parameters numerically, estimations using (second order) perturbation theory for these eigenvalue differences could be used as an alternative. There are thus three ways to find the influence that the parameters in the Hamiltonian have on its eigenvalue differences.

- Finding the eigenvalues analytically and use that to find expressions for the parameters.
- Vary a parameter for multiple measurements and see how the measurements change.
- Approximating the eigenvalues with perturbation theory to get a simplified expression to find approximated expressions for the parameters.

Perturbation theory might be preferred since it not only simplifies the calculations, but it can also give us insight into how the parameters influence the measurements.
In order to see how good of an approximation perturbation theory gives, the approximations of the eigenvalue differences for one specific will be compared to both the analytic expressions (if possible) and the exact values. The exact values for the eigenvalue differences are found by finding the eigenvalues of the Hamiltonian numerically using a script. The used values for the parameters can be found in Appendix C.

3 Perturbation Theory

Perturbation theory uses the solution of a simplified problem to approximate the solution of a more complex problem caused by a 'perturbation'. For us, this means that by writing the Hamiltonian as $\mathcal{H} = \mathcal{H}_0 + x\mathcal{H}'$, where $\mathcal{H}_0$ is the simplified matrix (usually a diagonal matrix) and $\mathcal{H}'$ is the 'perturbation' matrix caused by the parameter x, using the eigenvalues of $\mathcal{H}_0$ we can find an approximation of the eigenvalues of $\mathcal{H}$ in terms of x. However, it is not trivial that such approximations are possible or even exist in some cases. For that we need to make some assumptions for $\mathcal{H}$, where the importance of these assumptions will be clear in the derivation. In the following sections, first a part of perturbation theory will be formally derived, where in the second part we will take a simplified approach to the derivation.

3.1 Formal Perturbation Theory Derivation

In this section, we will show that an $n \times n$ matrix A, with real eigenvalues λ that are power series in some perturbation parameter ϵ and are convergent for small $|\epsilon|$ and can have a multiplicity greater than one, has corresponding eigenvectors u, where its elements u_i, $i = 1, \ldots, n$ are also power series in ϵ and convergent for small ϵ. This is the foundation for the approximations we will be able to make, because knowing that we can write the exact eigenvalues of $\mathcal{H}$ as convergent power series, we can use a finite amount of terms as our approximation. The following proof is based on the proof in *Perturbation Theory of Eigenvalue Problems* by Franz Rellich [3], where the full derivation of Perturbation Theory can be found.

Let the metric space be a Hilbert space. Suppose we have the eigenvalue problem $Au = \lambda u$, where A is Hermitian square $n \times n$ matrix and has elements a_{ij} which are power series in the perturbation parameter ϵ which are convergent for small $|\epsilon|$, λ is the eigenvalue corresponding to eigenvector u, and all eigenvectors of A are orthonormal. We can find the eigenvalues by solving the equation $\det(A - \lambda I) = 0$, with I the $n \times n$ identity matrix. Finding λ requires solving the polynomial

$$\lambda^n + c_1\lambda^{n-1} + \cdots + c_n = 0,$$

where c_i, $i = 1, \ldots, n$ depends on ϵ and which converge for small $|\epsilon|$.
We can write the solutions to this polynomial as power series,

$$\lambda(\epsilon) = a_0 + a_1\epsilon + \ldots. \tag{1}$$

Then for such an eigenvalue, we need to show that there exists an eigenvector $u(\epsilon) = (u_1(\epsilon), u_2(\epsilon), \ldots, u_n(\epsilon))$, where each $u_i(\epsilon)$, $i = 1, \ldots, n$ converges for small $|\epsilon|$ and $||u(\epsilon)|| = 1$. In other words, we need to show that this vector $u(\epsilon)$ is a solution for the equation

$$\sum_{k=1}^{n} a_{ik}(\epsilon)u_k(\epsilon) = \lambda(\epsilon)u_i(\epsilon), \quad i = 1, \ldots, n.$$

To prove this, we first need some definitions and prove the following lemma.

Definition 1. Given a matrix M, the (i,j) **minor** of M is obtained by removing the i'th row and j'th column of M.

Definition 2. The **cofactor** M_{ij} of a matrix M is the determinant of the (i,j) minor of M.

Definition 3. The **spectrum** of a matrix M is the set of all eigenvalues of M.

Lemma 1. Let $\gamma_{ik}(\epsilon)$, $i, k = 1, \ldots, n$ denote the elements of an $n \times n$ matrix which are all power series convergent in a neighbourhood of $\epsilon = 0$, and let

$$\det(\gamma_{ik})_{i,k=1,\ldots,n} = 0.$$

Then there exists a vector

$$\alpha(\epsilon) = (\alpha_1(\epsilon), \ldots, \alpha_n(\epsilon)) \tag{2}$$

where its elements are power series which are convergent in a neighbourhood of $\epsilon = 0$ such that

$$\sum_{k=1}^{n} \gamma_{ik}(\epsilon)\alpha_k(\epsilon) = 0$$

and for $\epsilon \in \mathbb{R}$ we have that $||\alpha(\epsilon)||^2 = 1$, so

$$\sum_{k=1}^{n} |\alpha_k(\epsilon)|^2 = 1.$$

Proof. First of all, if all elements $\gamma_{ik}(\epsilon) = 0$ for $i, k = 1, \dots, n$, then it is trivial that we can take any normed vector with constants as elements as $\alpha(\epsilon)$.
Let's assume that not all γ_{ik} are zero. Then there exists an integer r with $1 \leq r \leq n-1$ such that a $r \times r$ minor determinant of the matrix is non-zero, but every $r+1$ minor vanishes. Then we can assume without loss of generality that

$$\det(\gamma_{ik})_{i,k=1,\dots,r} \neq 0.$$

Let us denote $\Gamma_{ki}(\epsilon)$ as the cofactor of $\gamma_{ik}(\epsilon)$ in the determinant

$$\det(\gamma_{ik})_{i,k=1,\dots,r+1},$$

and let us define the vector $f(\epsilon)$ with elements

$$f_k(\epsilon) = \begin{cases} \Gamma_{k,r+1} & \text{for } k = 1, \dots, r+1, \\ 0 & \text{for } k = r+2, \dots, n. \end{cases}$$

Note that all f_k, $k = 1, \dots, n$ are power series in ϵ that are convergent for small $|\epsilon|$. Also note that

$$\sum_{k=1}^{n} \gamma_{ik}(\epsilon) f_k(\epsilon) = \sum_{k=1}^{r+1} \gamma_{ik}(\epsilon)\Gamma_{k,r+1}(\epsilon) = 0, \quad i = 1, \dots, n.$$

The last equality holds, because this summation can be interpreted as finding the determinant of the matrix of the elements γ_{ik}, $i, k = 1, \dots, r+1$ and we have assumed that every $r+1$ minor determinant is zero.
From $f(\epsilon)$ we can now construct $\alpha(\epsilon)$,

$$\alpha(\epsilon) = \frac{f(\epsilon)}{||f(\epsilon)||}.$$

Recall that the elements of $f(\epsilon)$ are convergent power series in ϵ and real for $\epsilon \in \mathbb{R}$. Then the norm can be written as formal Laurent series:

$$||f(\epsilon)||^2 = |f_1(\epsilon)|^2 + |f_2(\epsilon)|^2 + \dots + |f_n(\epsilon)|^2 = \epsilon^{2m}(b_0 + b_1\epsilon + \dots), \quad b_0 \neq 0, m \in \mathbb{Z},$$

where m is the order of the series. Then the norm can be written as

$$||f(\epsilon)|| = \epsilon^m(d_0 + d_1\epsilon + \dots).$$

The elements of $\alpha(\epsilon)$ are then given by

$$\alpha_k(\epsilon) = \frac{f_k(\epsilon)}{\epsilon^m(d_0 + d_1\epsilon + \dots)}, \quad k = 1, \dots, n.$$

Since every $f_k(\epsilon)$ has order m, every $\alpha_k(\epsilon)$ is analytic for small $|\epsilon|$ which means they can be written as convergent power series. Also, $||\alpha(\epsilon)|| = 1$. Therefore we shown the existence of the vector $\alpha(\epsilon)$ that has the properties as in the lemma. □

With this lemma we can prove the theorem that proves the existence of an eigenvector $u(\epsilon)$ where its elements are convergent power series in $|\epsilon|$ for a given eigenvalue $\lambda(\epsilon) = a_0 + a_1\epsilon + \dots$.

Theorem 1. Suppose elements $a_{ik}(\epsilon)$, $i,k = 1,\dots,n$ of Hermitian matrix $A(\epsilon)$ are convergent power series in a neighbourhood around $\epsilon = 0$ and real for $\epsilon \in \mathbb{R}$. Suppose $\lambda = \lambda(0)$ is an eigenvalue of matrix $A = A(0)$ with multiplicity $h > 1$ and suppose the interval $(\lambda - d_1, \lambda + d_2)$ with $d_1, d_2 \in \mathbb{R}_{\geq 0}$ contain no other eigenvalues of A other than λ.
Then there exist power series

$$\begin{aligned} &\lambda_1(\epsilon),\dots,\lambda_2(\epsilon), \\ &f_1^{(\nu)}(\epsilon),\dots,f_n^{(\nu)}(\epsilon), \quad \nu = 1,\dots,h, \end{aligned}$$

that are convergent in a neighbourhood of $\epsilon = 0$, which satisfy the following conditions:

1. The vector $\phi^{(\nu)} = (f_1^{(\nu)}(\epsilon),\dots,f_n^{(\nu)}(\epsilon))$ is an eigenvector of $A(\epsilon)$ belonging to the eigenvalue $\lambda_\nu(\epsilon)$, with $\lambda_\nu(0) = \lambda$ and for $\epsilon \in \mathbb{R}$ all the eigenvectors are orthonormal,

$$\langle \phi^{(\nu)}(\epsilon), \phi^{(\mu)}(\epsilon)\rangle = \delta_{\nu\mu}, \quad \nu,\mu = 1,\dots,h.$$

2. For each pair of $d_1', d_2' \in \mathbb{R}_{\geq 0}$, with $d_1' < d_1$ and $d_2' < d_2$, there exists $\rho \in \mathbb{R}_{\geq 0}$ such that the spectrum of $A(\epsilon)$ in the interval $[\lambda - d_1', \lambda + d_2']$ consists of the points $\lambda_1(\epsilon),\dots,\lambda_h(\epsilon)$ if $|\epsilon| < \rho$.

Proof. In Lemma 1 we have proved condition 1 of the theorem in the case when $h = 1$. If we assume that the theorem holds for $h-1$, then by using induction, we can prove it for h.
Assume the theorem holds for $h-1$. From Lemma 1, we know there exists a vector $\phi^{(1)}(\epsilon) = (f_1^{(1)}(\epsilon),\dots,f_n^{(1)}(\epsilon))$, where its elements are power series of ϵ and convergent for $|\epsilon|$ small. We define the matrix $P(\epsilon)$ such that

$$P(\epsilon)u = \langle \phi^{(1)}, u\rangle \phi^{(1)},$$

with elements $p_{ik}(\epsilon) = f_i^{(1)}(\epsilon)\overline{f_k^{(1)}(\epsilon)}$, $i,k = 1,\dots,n$. Let us define $B(\epsilon) = A(\epsilon) - P(\epsilon)$, which has elements $b_{ik}(\epsilon) = a_{ik}(\epsilon) - p_{ik}(\epsilon)$. Note that $b_{ik}(\epsilon)$ are power series in ϵ that are convergent for small $|\epsilon|$ and note that the matrix $B(\epsilon)$ is Hermitian.
Define $\psi_1 = \phi^{(1)}(0)$ and take vectors $\psi_1,\dots,\psi_h$ the set of orthonormal vectors belonging to the same eigenvalue $\lambda = \lambda(0)$ of $A = A(0)$. Then we have that for $j = 2,\dots,n$,

$$B(0)\psi_j = A(0)\psi_j - P(0)\psi_j = \lambda\psi_1 - \langle \psi_j, \psi_1\rangle\psi_j = \lambda\psi_j.$$

Since this holds for $j = 2,\dots,n$, λ is an eigenvalue of $B(0)$ with multiplicity of at least $h-1$.

Now we if we can prove that the multiplicity is exactly $h-1$, then we know what the first part of the theorem holds for $B(\epsilon)$. From there we can show that it also holds for $A(\epsilon)$.

Assume that the multiplicity is greater than $h-1$. Then there should exist a vector ψ with $||\psi|| = 1$ such that $B(0)\psi = \lambda\psi$ and $\langle \psi, \psi_j\rangle = 0$ for $j = 2,\dots,h$. We know that

$$\begin{aligned} B(0)\psi_1 &= A(0)\psi_1 - P(0)\psi_1 \\ &= \lambda\psi_1 - \langle \psi_1, \psi_1\rangle\psi_1 \\ &= (\lambda - 1)\psi_1 \end{aligned}$$

Then we must have that $\langle \psi, \psi_1\rangle = 0$, because then the multiplicity is greater than $h-1$. Therefore,

$$\begin{aligned} A(0)\psi &= B(0)\psi + P(0)\psi \\ &= \lambda\psi + \langle \psi_1, \psi\rangle\psi_1 \\ &= \lambda\psi. \end{aligned}$$

This means that ψ is also an eigenvector of $A(0)$ and that all the eigenvectors $\psi, \psi_1, \ldots, \psi_n$ are orthogonal. Then the eigenvalue λ of $A(0)$ has multiplicity $h+1$, which is a contradiction. Thus, the multiplicity of λ from $B(0)$ cannot excede $h-1$.

Now we know the first part of the theorem holds for $B(\epsilon)$, we can say that there exist power series $\lambda_\nu(\epsilon)$ and $f_1^{(\nu)}(\epsilon), \ldots, f_n^{(\nu)}(\epsilon)$ for $\nu = 2, \ldots, h$ in ϵ, such that they are all convergent in a neighbourhood of $\epsilon = 0$ and the vector $\phi^{(\nu)} = (f_1^{(\nu)}, \ldots, f_n^{(\nu)})$ is an eigenvector of $B(\epsilon)$ with eigenvalue $\lambda_\nu(\epsilon)$ with $\lambda_\nu(0) = \lambda$ and for $\epsilon \in \mathbb{R}$, all the eigenvectors are orthonormal, so $\langle \phi^{(\nu)}, \phi^{(\mu)} \rangle = \delta_{\nu\mu}$ for $\nu, \mu = 2, \ldots, h$.

We know from Lemma 1 that $\phi^{(1)}(\epsilon) = (f_1^{(1)}, \ldots, f_n^{(1)})$ is an eigenvector of $A(\epsilon)$ with eigenvalue $\lambda_1(\epsilon)$, so $A(\epsilon)\phi^{(1)}(\epsilon) = \lambda_1(\epsilon)\phi^{(1)}(\epsilon)$. Then $B(\epsilon)\phi^{(1)}(\epsilon) = (\lambda_1(\epsilon) - 1)\phi^{(1)}(\epsilon)$.

For small $|\epsilon|$, $\lambda_\nu(\epsilon) \neq \lambda_1(\epsilon) - 1$, so $\langle \phi^{(\nu)}, \phi^{(1)} \rangle = 0$. If not we would have that $\langle \phi^{(\nu)}, \phi^{(1)} \rangle = 1$ since $||\phi^{(1)}(\epsilon)||^2 = 1$, but then $\lambda_\nu(\epsilon) = \lambda_1(\epsilon) - 1$ which is false. Then for $\nu = 2, \ldots, h$,

$$\begin{aligned} A(\epsilon)\phi^{(\nu)} &= B(\epsilon)\phi^{(\nu)} + P(\epsilon)\phi^{(\nu)} \\ &= \lambda_\nu(\epsilon)\phi^{(\nu)} + \langle \phi^{(1)}, \phi^{(\nu)} \rangle \phi^{(1)} \\ &= \lambda_\nu(\epsilon)\phi^{(\nu)}(\epsilon). \end{aligned}$$

Then indeed, the vectors $\phi^{(\nu)}(\epsilon)$ are eigenvectors of $A(\epsilon)$ belonging to the eigenvalues $\lambda_\nu(\epsilon)$ for $\nu = 1, \ldots, h$, where $\langle \phi^{(\nu)}(\epsilon), \phi^{(\mu)}(\epsilon) \rangle = \delta_{\nu\mu}$, $\nu, \mu = 1, \ldots, h$. Therefore we have proven the first part of the theorem.

The second part of the theorem is nearly trivial, as for all eigenvalues of $A(\epsilon)$, we have that $\lambda_i(|\epsilon|) \to \lambda$ for $i = 1, \ldots, h$, since $\lambda_i(0) = \lambda$ and all $\lambda_i(\epsilon)$ are convergent power series in ϵ. □

Now we have formally proven that for a hermitian $n \times n$ matrix A with elements that are convergent power series in some (small) variable ϵ has eigenvalues $\lambda(\epsilon)$ with corresponding eigenvectors $u(\epsilon)$ with elements that are all convergent power series in ϵ. Using this knowledge, we can possibly approximate the eigenvalues of $A(\epsilon)$ by taking a finite amount of elements.

3.2 Simplified Perturbation Theory Derivation

For the simplified derivation, we will assume that the multiplicity is 1 for all eigenvalues of the Hamiltonian H. Note how in equations 1 and 2, the eigenvalues and eigenvectors of H can be written as power series, which was proven to be possible in the previous subsection. Indeed, in our final approximation for the eigenvalues, we only consider the first three elements of both power series. This is referred to as 'second order' perturbation theory.

The following practical derivation will result in explicit equations which will be used to approximate the eigenvalues of the Hamiltonian. This derivation can also be found in David J. Griffith's *Introduction to Quantum Mechanics* [4].

We start by splitting the Hamiltonian into two parts. One part consists of a diagonal matrix and the second part represents a perturbation that changes the eigenvalues of the system. If we call our Hamiltonian H, an $m \times m$ matrix, we can write it as

$$H = H_0 + \lambda H'. \tag{3}$$

H_0 describes the unperturbed system and has eigenvalues E_n^0 and eigenvectors ϕ_n^0. H' is the perturbation, with λ indicating the order of the correction. We can write the eigenvalues E_n and the eigenvectors ϕ_n of H as power series in λ. Then we get

$$\begin{aligned} E_n &= E_n^0 + \lambda E_n^1 + \lambda^2 E_n^2 + \ldots \lambda^i E_n^i + \ldots \\ \phi_n &= \phi_n^0 + \lambda \phi_n^1 + \lambda^2 \phi_n^2 + \ldots \lambda^i \phi_n^i + \ldots \end{aligned}$$

Here, i shows the order of the correction. If we substitute this into H, we get the following result:

$$\begin{aligned} H\phi_n &= (H^0 + \lambda H')\phi_n \\ &= (H^0 + \lambda H')(\phi_n^0 + \lambda\phi_n^1 + \lambda^2\phi_n^2 + \dots) \\ &= H^0\phi_n^0 + \lambda(H^0\phi_n^1 + H'\phi_n^0) + \lambda^2(H^0\phi_n^2 + H'\phi_n^1) + \dots \\ &= E_n\phi_n \\ &= (E_n^0 + \lambda E_n^1 + \lambda^2 + E_n^2 + \dots)(\phi_n^0 + \lambda\phi_n^1 + \lambda^2\phi_n^2 + \dots) \\ &= E_n^0 + \lambda(E_n^0\phi_n^1 + E_n^1\phi_n^0) + \lambda^2(E_n^0\phi_n^2 + E_n^1\phi_n^1 + E_n^2\phi_n^0) + \dots \end{aligned} \tag{4}$$

Re-writing this gives the equation below.

$$\begin{aligned} &H^0\phi_n^0 + \lambda(H^0\phi_n^1 + H'\phi_n^0) + \lambda^2(H^0\phi_n^2 + H'\phi_n^1) + \dots = \\ &E_n^0 + \lambda(E_n^0\phi_n^1 + E_n^1\phi_n^0) + \lambda^2(E_n^0\phi_n^2 + E_n^1\phi_n^1 + E_n^2\phi_n^0) + \dots \end{aligned} \tag{5}$$

Then first order terms together give equation 6 where taking the inner products with ϕ_n^0 with both sides results in equation 7

$$H^0\phi_n^1 + H'\phi_n^0 = E_n^0\phi_n^1 + E_n^1\phi_n^0 \tag{6}$$

$$\langle\phi_n^0|H^0|\phi_n^1\rangle + \langle\phi_n^0|H'|\phi_n^0\rangle = E_n^0\langle\phi_n^0|\phi_n^1\rangle + E_n^1 \tag{7}$$

By re-arranging equation 7 the first-order correction to the energy is shown below.

$$E_n^1 = \langle\phi_n^0|H^0|\phi_n^1\rangle + \langle\phi_n^0|H'|\phi_n^0\rangle - E_n^0\langle\phi_n^0|\phi_n^1\rangle$$

Since the Hamiltonian is always Hermitian, the resulting equation for the first order correction is given by

$$E_n^1 = \langle\phi_n^0|H'|\phi_n^0\rangle\,. \tag{8}$$

To find the second order correction, we can write equation 6 as

$$(H^0 - E_n^0)\psi_n^1 = -(H' - E_n^1)\psi_n^0. \tag{9}$$

Using the above equation we can find ψ_n^1. This is an inhomogeneous differential equation for ψ_n^1 and the solution is a linear combination of all the unperturbed wave functions.

$$\psi_n^1 = \sum_{m\neq n} c_m^{(n)}\psi_m^0 \tag{10}$$

To determine $c_m^{(n)}$, ψ_n^1 is plugged into equation 9 and taking the inner product with ψ_l^0 due to orthogonality we find

$$c_m^{(n)} = \frac{\langle\psi_m^0|H'|\psi_n^0\rangle}{(E_n^0 - E_m^0)}. \tag{11}$$

Using the second order terms from equation 5 and taking the inner product with ψ_n^0 gives

$$\langle\psi_n^0|H^0|\psi_n^2\rangle + \langle\psi_n^0|H'|\psi_n^1\rangle = E_n^0\langle\psi_n^0|\psi_n^2\rangle + E_n^1\langle\psi_n^0|\psi_n^1\rangle + E_n^2\langle\psi_n^0|\psi_n^0\rangle\,.$$

Using equations 10, 11, that H^0 is Hermitian, $\langle\psi_n^0|\psi_n^0\rangle = 1$ and that $\langle\psi_n^0|\psi_n^1\rangle = 0$, we find the second order correction E_n^2 to the energies:

$$E_n^2 = \sum_{m\neq n}\frac{|\langle\phi_m^0|H'|\phi_n^0\rangle|^2}{E_n^0 - E_m^0}. \tag{12}$$

Since λ is small, we will only consider the first two orders of corrective eigenvalues. Then, using equations 8 and 12, the approximation for the eigenvalues of H will thus be

$$E_n = E_n^0 + \langle\phi_n^0|\,H'\,|\phi_n^0\rangle + \sum_{m\neq n}\frac{|\langle\phi_m^0|\,H'\,|\phi_n^0\rangle|^2}{E_n^0 - E_m^0}. \tag{13}$$

Note that if the eigenvalues of H^0 are close, $E_n^0 - E_m^0$ is very small and then the second order correction to E_n will be very large, and perturbation theory will no longer give an accurate approximation.

4 System of the Electron Spin

In the simplest case, we only consider the electron spin, where the elements of the Hamiltonian $\mathcal{H}$ only depend on the zero-field splitting Δ_{ZFS}, the gyromagnetic ratio γ_e and a magnetic field denoted by $(B_z, B_\perp)$, where B_z is the magnitude of the magnetic field along the $\hat{\mathbf{z}}$ direction, and $B_\perp$ is the magnitude of the magnetic field perpendicular to $\hat{\mathbf{z}}$. This magnetic field is applied to lift the degeneracy of the excited states due to the Zeeman effect, i.e. the multiplicity of the eigenvalues of $\mathcal{H}$ are 1. The presence of $B_\perp$ changes the eigenvalues in regard to a system where $B_\perp$ is absent. Aligning the field such that $B_\perp = 0$ will simplify the problem of finding the eigenvalue differences. We want to know how the eigenvalues depend on $B_\perp$ so we can align the magnetic field to the NV axis (so $B_\perp = 0$).

4.1 Magnetic fields expressed in measured energy differences.

The Hamiltonian of this system is given below, where the operators $\hat{\mathbf{S}}_z$ and $\hat{\mathbf{S}}_x$ are the spin matrices as shown in equations 16. For simplicity, we take $\hbar = 1$ throughout the entire report. From the Hamiltonian, we want to find expressions for the magnetic field $(B_z, B_\perp)$ and the electron zero-field splitting Δ_{ZFS}. Note that we cannot extract the electron gyromagnetic ratio γ_e in this problem, as this is always multiplied by the magnetic field. Therefore, $\gamma_e B_z$ is considered as a single parameter. The method of extraction of Δ_{ZFS} and B_z is close to the method as in the supplementary to [6].

$$\mathcal{H} = \Delta_{ZFS}(\hat{\mathbf{S}}_z)^2 + \gamma_e B_z \hat{\mathbf{S}}_z + \gamma_e B_\perp \hat{\mathbf{S}}_x \tag{14}$$

$$= \begin{bmatrix} \Delta_{ZFS} + \gamma_e B_z & \frac{\gamma_e B_\perp}{\sqrt{2}} & 0 \\ \frac{\gamma_e B_\perp}{\sqrt{2}} & 0 & \frac{\gamma_e B_\perp}{\sqrt{2}} \\ 0 & \frac{\gamma_e B_\perp}{\sqrt{2}} & \Delta_{ZFS} - \gamma_e B_z \end{bmatrix} \tag{15}$$

$$\hat{\mathbf{S}}_z = \hbar \begin{bmatrix} 1 & 0 & 0 \\ 0 & 0 & 0 \\ 0 & 0 & -1 \end{bmatrix}, \quad \hat{\mathbf{S}}_x = \frac{\hbar}{\sqrt{2}} \begin{bmatrix} 0 & 1 & 0 \\ 1 & 0 & 1 \\ 0 & 1 & 0 \end{bmatrix} \tag{16}$$

The reason the $\hat{\mathbf{S}}_y$ operator is not present in $\mathcal{H}$ is because for now the orientation of the perpendicular magnetic field $B_\perp$ is irrelevant and such, without loss of generality, we can take this to be along $\hat{\mathbf{x}}$.

The eigenvalues of the matrix $\mathcal{H}$ are the eigenenergies corresponding to the different spin states m_s of the electron. The change in frequency due to spin transitions from the ground state to one of the excited states are measurable. The energy differences are denoted as $\omega_\pm$ for the spin transitions $m_s = 0 \leftrightarrow \pm 1$, where $\omega_+ > \omega_-$, and the frequency differences are denoted as $f_\pm = \frac{\omega_\pm}{2\pi}$. Since ω_+ and ω_- are measurable, we want to express $(\gamma_e B_z, \gamma_e B_\perp)$ and Δ_{ZFS} as functions of ω_+ and ω_-. Because the frequency differences of the electron spin transitions are measurable, the eigenvalues of $\mathcal{H}$ are written as $\lambda_1 = \lambda_0$, $\lambda_2 = \lambda_0 + \omega_+$ and $\lambda_3 = \lambda_0 + \omega_-$. Then by finding the eigenvalues, we can find expressions for ω_+ and ω_-.

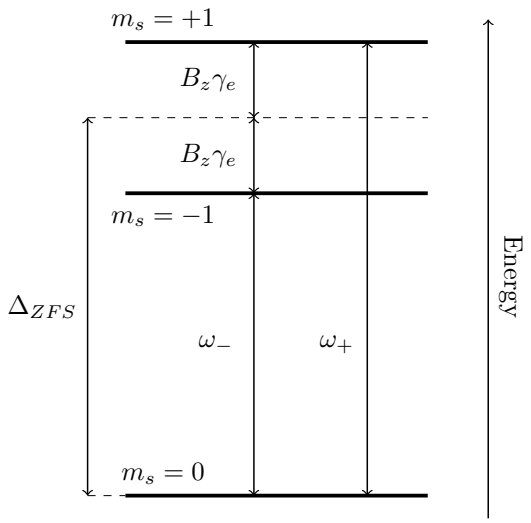

Figure 2: Energy levels for different spin states m_s in absence of $B_\perp$. $\omega_\pm$ are the difference in energies between the ground state and the ± 1 spin states, where we take $\omega_+ > \omega_-$ as a convention. In practice, a frequency difference f between electron spin transitions is measured, which is related to the energy differences by $\omega_\pm = 2\pi f_\pm$. For $B_\perp = 0$, parameters Δ_{ZFS} and $\gamma_e B_z$ can be calculated with equations 18 and 19.

If $B_\perp$ is set to zero, the energy levels of the electron for different spin states are shown in Figure 2.
$\mathcal{H}(B_\perp = 0) = \mathcal{H}_0$ is given by equation 17. The eigenvalues of $\mathcal{H}_0$ are the values on the diagonal of the matrix, and thus it follows that $\omega_\pm = \Delta_{ZFS} \pm \gamma_e B_z$, where we take that $B_z > 0$ since $\omega_+ > \omega_-$. Then we can extract the expressions for Δ_{ZFS} and $\gamma_e B_z$, shown in equations 18 and 19.

$$\mathcal{H}_0 = \begin{bmatrix} \Delta_{ZFS} + \gamma_e B_z & 0 & 0 \\ 0 & 0 & 0 \\ 0 & 0 & \Delta_{ZFS} - \gamma_e B_z \end{bmatrix} \tag{17}$$

$$\Delta_{ZFS} = \frac{1}{2}(\omega_+ + \omega_-) \tag{18}$$

$$\gamma_e B_z = \frac{1}{2}(\omega_+ - \omega_-) \tag{19}$$

In reality it might be that $B_\perp \neq 0$. Then $\mathcal{H}$ as shown in equation 15 has off-diagonal terms, which makes finding its eigenvalues less trivial. We will now find expressions for the parameters in $\mathcal{H}$ for $B_\perp \neq 0$.

To find λ_1, λ_2 and λ_3, we have to solve $||\mathcal{H} - \lambda_i I_r|| = 0$, where I_3 is the 3×3 identity matrix. This means that there are three polynomials as in equation 20 which have to be solved for each λ_i.

$$-B_\perp^2 \Delta_{ZFS} \gamma_e^2 + B_\perp^2 \gamma_e^2 \lambda_i + B_z^2 \gamma_e^2 \lambda_i - \Delta_{ZFS}^2 \lambda_i + 2\Delta_{ZFS} \lambda_i^2 - \lambda_i^3 = 0 \tag{20}$$

Instead of solving this third degree polynomial for eigenvalues λ_i which we cannot measure anyway, it is better to find expressions for the eigenvalue differences ω_+ and ω_-. First we find expressions for B_z and $B_\perp$, and eliminate λ_0 from the equations. This results in the expressions in equations 21a-21b. From the assumption that $B_z > 0$, the solution is the positive square root. For $B_\perp$, the solution can be either positive or negative.

$$B_z^2 = \frac{-(\Delta_{ZFS} - 2\omega_+ + \omega_-)(\Delta_{ZFS} + \omega_- + \omega_+)(\Delta_{ZFS} - 2\omega_- + 2\omega_+)}{27\gamma_e^2 \Delta_{ZFS}} \tag{21a}$$

$$B_\perp^2 = \frac{-(2\Delta_{ZFS} - \omega_- - \omega_+)(2\Delta_{ZFS} + 2\omega_- - \omega_+)(2\Delta_{ZFS} - \omega_- + 2\omega_+)}{27\gamma_e^2 \Delta_{ZFS}} \tag{21b}$$

Up until now, the results for B_z and $B_\perp$ are exactly as in [6]. But the expressions for B_z and $B_\perp$ depend on the unknown parameter Δ_{ZFS} still. In [6], Δ_{ZFS} was approximated as in equation 18. But we only take this to be a good estimate if we manage to set $B_\perp = 0$. In that case, $B_\perp$ is a known parameter and then we can extract both $\gamma_e B_z$ and Δ_{ZFS} from the two equations 19 and 18.

Still, using the expressions of B_z and $B_\perp$ to find ω_+ and ω_- directly is difficult. By substituting average $\bar{\omega}$ and difference $\delta\omega$ (shown below) in B_z and $B_\perp$, we find analytic expressions for ω_- and ω_+ using equations 24a-24b.

$$\bar{\omega} = \frac{\omega_+ + \omega_-}{2} \tag{22}$$

$$\delta\omega = \frac{\omega_+ - \omega_-}{2} \tag{23}$$

First solving for $\bar{\omega}$ and $\delta\omega$ simplifies equations 21a-21b and the substitution is shown below.

$$B_z^2 = \frac{-\Delta_{ZFS}^3 + 3\Delta_{ZFS}\bar{\omega}^2 - 2\bar{\omega}^3 + 9\Delta_{ZFS}(\delta\omega)^2 + 18\bar{\omega}(\delta\omega)^2}{27\gamma_e^2\Delta_{ZFS}} \tag{24a}$$

$$B_\perp^2 = \frac{-8\Delta_{ZFS}^3 + 6\Delta_{ZFS}\bar{\omega}^2 + 2\bar{\omega}^3 + 18\Delta_{ZFS}(\delta\omega)^2 - 18\bar{\omega}(\delta\omega)^2}{27\gamma_e^2\Delta_{ZFS}} \tag{24b}$$

The resulting equations for $\bar{\omega}$ and $\delta\omega$ are 25-26, simplified using some new functions in equations 27a-27b.

$$\bar{\omega} = 2^{-\frac{1}{3}}\mathrm{Re}\left[(F + \sqrt{F^2 - 4G^3})^{\frac{1}{3}}\right] \tag{25}$$

$$\delta\omega = 2^{-\frac{1}{3}}3^{-\frac{1}{2}}\mathrm{Im}\left[(F + \sqrt{F^2 - 4G^3})^{\frac{1}{3}}\right] \tag{26}$$

$$F(B_z, B_\perp) = \Delta_{ZFS}(3^2\gamma^2(B_\perp^2 - 2B_z^2) + 2\Delta_{ZFS}^2) \tag{27a}$$

$$G(B_z, B_\perp) = 3\gamma^2(B_\perp^2 + B_z^2) + \Delta_{ZFS}^2 \tag{27b}$$

The increase of both $\bar{\omega}$ and $\delta\omega$ are plotted as a function of $B_\perp$ for a specific case in figure 3 using values for the parameters as in Appendix C. Below both plots, the difference between the exact values for $\bar{\omega}$ and $\delta\omega$ and the analytic functions is plotted. $e(x)$ here is defined as the difference between the eigenfrequency differences found analytically or approximated ($F(x)$) with the eigenfrequency differences of the Hamiltonian found numerically using a script ($F(x)_{ex}$), so $e(x) = F(x)_{ex} - F(x)$. This difference is a few μHz at its highest for $B_\perp$ between -10 and 10 Gauss. But this should actually be zero, so this non-zero difference is most likely due to machine precision

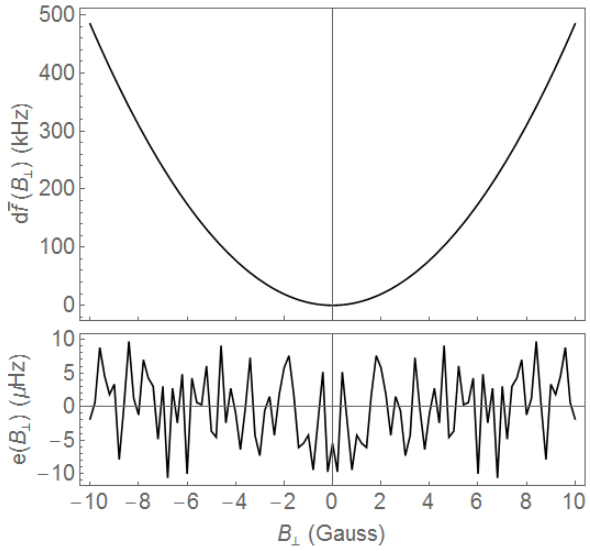

(a) Increase of the average of the frequency differences for electron spin transition $m_s = 0 \leftrightarrow \pm 1$.

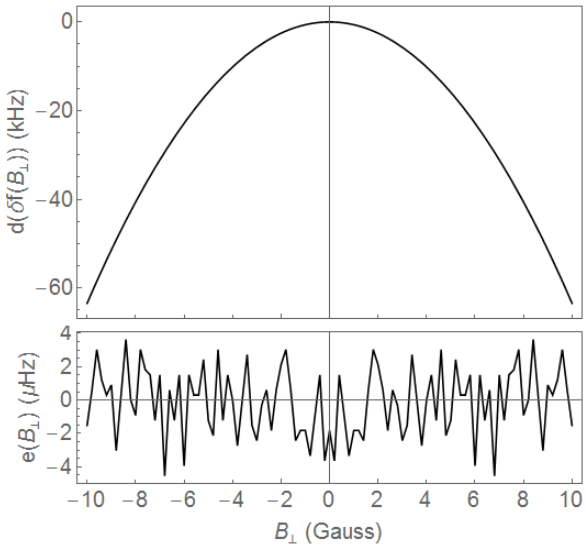

(b) Increase in difference of the frequency differences for electron spin transition $m_s = 0 \leftrightarrow \pm 1$.

Figure 3: These graphs show the increase of the average and difference of the frequency differences for both spin transitions from the ground state to the excited states. Since $f_\pm = \frac{\omega_\pm}{2\pi}$ are measurable, we use the notations $\bar{f} = \frac{\bar{\omega}}{2\pi}$ and $\delta f = \frac{\delta\omega}{2\pi}$, where $d\bar{f}(B_\perp) = \bar{f}(B_\perp) - \bar{f}(0)$ and $d(\delta f(B_\perp)) = \delta f(B_\perp) - \delta f(0)$ are the increase of $\bar{f}$ and δf for different $B_\perp$. Both graphs show parabolic behaviour, where (a) is at its minimum and (b) is at its maximum for $B_\perp = 0$. Below each graph, the difference between the analytic and exact values, $e(B_\perp)$, is plotted for $\bar{f}$ and δf . The magnitude of these are in μHz and non-zero. Since $e(B_\perp)$ is very small in comparison with the frequencies $\bar{f}$ and δf (in GHz), this is most likely due to machine precision.

From $\bar{\omega}$ and $\delta\omega$ we can then retrieve expressions for ω_+ and ω_-, where we either take the positive or negative solution of $\delta\omega$ such that $\omega_+ > \omega_-$ (equations 28). ω_+ and ω_- are shown in figure 4 as functions of $B_\perp$.

$$\begin{aligned}\omega_+ &= 2^{-\frac{1}{3}}\left(\mathrm{Re}\left[(F+\sqrt{F^2-4G^3})^{\frac{1}{3}}\right] + 3^{-\frac{1}{2}}\mathrm{Im}\left[(F+\sqrt{F^2-4G^3})^{\frac{1}{3}}\right]\right)\\ \omega_- &= 2^{-\frac{1}{3}}\left(\mathrm{Re}\left[(F+\sqrt{F^2-4G^3})^{\frac{1}{3}}\right] - 3^{-\frac{1}{2}}\mathrm{Im}\left[(F+\sqrt{F^2-4G^3})^{\frac{1}{3}}\right]\right)\end{aligned} \tag{28}$$

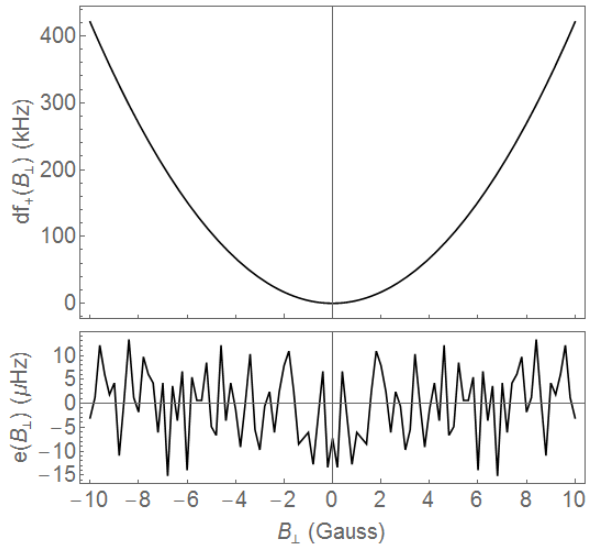

(a) Increase in frequency difference for electron spin transition $m_s = 0 \rightarrow +1$.

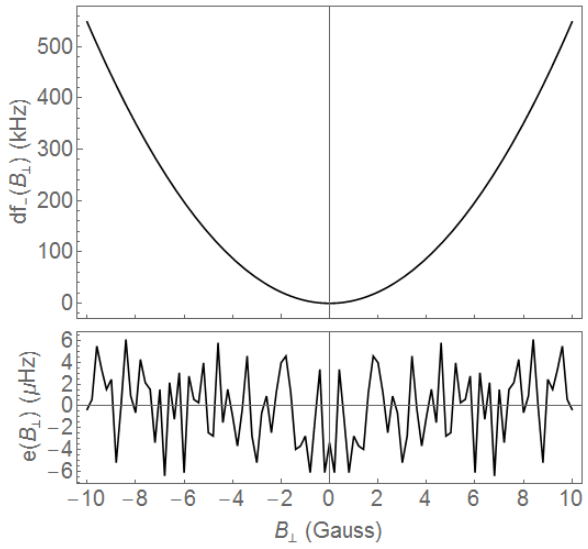

(b) Increase in frequency difference for electron spin transition $m_s = 0 \rightarrow -1$.

Figure 4: The above graphs show the increase of the frequency differences of the spin transitions as functions of the perpendicular magnetic field. Both graphs show parabolic behaviour, where both frequency differences are at their minimum for $B_\perp = 0$. Below each graph, $e(B_\perp)$ is plotted. Just as in figure 3, the magnitude of $e(B_\perp)$ is very small compared to the frequencies (in GHz).

To summarise the findings, we have found Δ_{ZFS} and $\gamma_e B_z$ if $B_\perp = 0$, but if $B_\perp \neq 0$, it is not possible to find all parameters as there are three parameters, but only two equations. Also, analytically finding the parameters of the Hamiltonian if $B_\perp \neq 0$ is possible, but it is a lengthy process due to the off-diagonal terms. From now on, we will only approximate these parameters.

4.2 Estimating the energy differences using second order perturbation theory.

In the previous subsection it was shown that the analytic functions for ω_+ and ω_- were time consuming to find, and it was not immediately clear how they depend on the parameters due to complexity of the expressions. Instead, we could also approximate these functions using (second order) perturbation theory. Since the system is non-degenerate due to the applied magnetic field, we can use the method as derived in 3.2, where the Hamiltonian elements proportional to the parameter $B_\perp$ will be treated as the perturbation. We start by splitting up $\mathcal{H}$ such as in equation 3, where $\mathcal{H}_0 = \mathcal{H}(B_\perp = 0)$ is given by equation 17 which is a simple diagonal matrix. The perturbation $\mathcal{H}'$ is then given by the equation below.

$$\mathcal{H}' = \gamma B_\perp \hat{\mathbf{S}}_x = \frac{\gamma B_\perp}{\sqrt{2}} \begin{bmatrix} 0 & 1 & 0 \\ 1 & 0 & 1 \\ 0 & 1 & 0 \end{bmatrix} \tag{29}$$

From $\mathcal{H}_0$ the eigenvalues can be read from the diagonal of the matrix in equation 17 which are the unperturbed energies. These three energies are denoted as E_i^0 in equations 30. These have corresponding eigenvectors which are given by equations 31

$$\begin{aligned} E_1^0 &= \Delta_{ZFS} + \gamma B_z \\ E_2^0 &= 0 \\ E_3^0 &= \Delta_{ZFS} - \gamma B_z \end{aligned} \tag{30}$$

$E_2^0 = 0$ is an allowed eigenvalue since $\mathrm{Det}(\mathcal{H}_0) = 0$, which means $\mathcal{H}_0$ has no inverse. Therefore, there exists an eigenvector belonging to the eigenvalue $E_2^0 = 0$. $\mathcal{H}_0$ has three eigenvectors corresponding to the ground

state and the two excited states.

$$|\psi_1^0\rangle = \begin{bmatrix}1\\0\\0\end{bmatrix}, \quad |\psi_2^0\rangle = \begin{bmatrix}0\\1\\0\end{bmatrix}, \quad |\psi_3^0\rangle = \begin{bmatrix}0\\0\\1\end{bmatrix} \tag{31}$$

The first-order corrections on the energies are calculated using the formula in equation 8. As a result, we find that all E_n^1 are zero. Now looking into the second-order corrections to the energies, we find non-zero corrections to the energies. Using equation 12, the second-order energy corrections are the sums below.

$$E_n^2 = \gamma^2 B_\perp^2 \sum_{m\neq n} \frac{|\langle\psi_m^0|\,\hat{\mathbf{S}}_x\,|\psi_n^0\rangle|^2}{E_n^0 - E_m^0}$$

All possible $\langle\psi_m^0|\,H'\,|\psi_n^0\rangle$ for $n, m = 1, 2, 3$, $n \neq m$ are shown below.

$$\langle\psi_2^0|\,\hat{\mathbf{S}}_x\,|\psi_1^0\rangle = \frac{1}{\sqrt{2}}\begin{bmatrix}0 & 1 & 0\end{bmatrix}\begin{bmatrix}0 & 1 & 0\\1 & 0 & 1\\0 & 1 & 0\end{bmatrix}\begin{bmatrix}1\\0\\0\end{bmatrix} = \frac{1}{\sqrt{2}}\begin{bmatrix}0 & 1 & 0\end{bmatrix}\begin{bmatrix}0\\1\\0\end{bmatrix} = \frac{1}{\sqrt{2}}$$

$$\langle\psi_1^0|\,\hat{\mathbf{S}}_x\,|\psi_2^0\rangle = \langle\psi_3^0|\,\hat{\mathbf{S}}_x\,|\psi_2^0\rangle = \langle\psi_2^0|\,\hat{\mathbf{S}}_x\,|\psi_3^0\rangle = \frac{1}{\sqrt{2}}$$

$$\langle\psi_3^0|\,\hat{\mathbf{S}}_x\,|\psi_1^0\rangle = \langle\psi_1^0|\,\hat{\mathbf{S}}_x\,|\psi_3^0\rangle = 0$$

Calculating E_n^2 for $n = 1, 2, 3$ using the above calculations will give the results below, and from there, we have found the second order corrections to the eigenenergies as shown in equations 33.

$$\begin{aligned} E_1^2 &= \frac{\gamma^2 B_\perp^2}{2(\Delta_{ZFS} + \gamma B_z)} \\ E_2^2 &= \frac{\Delta_{ZFS}\gamma^2 B_\perp^2}{\gamma^2 B_z^2 - \Delta_{ZFS}^2} \\ E_3^2 &= \frac{\gamma^2 B_\perp^2}{2(\Delta_{ZFS} - \gamma B_z)}. \end{aligned} \tag{32}$$

$$\begin{aligned} E_1 &\approx E_1^0 + E_1^2 \\ E_2 &\approx E_2^0 + E_2^2 \\ E_3 &\approx E_3^0 + E_3^2. \end{aligned} \tag{33}$$

Since E_1, E_2 and E_3 are the eigenvalues of $\mathcal{H}$, the measurable eigenvalue differences are then $\omega_+ = E_1 - E_0$ and $\omega_- = E_3 - E_0$. Using the approximations for the energies (equations 33), we have found approximations for $\omega_\pm$, denoted as $\omega'_\pm$ as given by the following equations:

$$\begin{aligned} \omega'_+ &= E_1^0 + E_1^2 - (E_2^0 + E_2^2) \\ &= \Delta_{ZFS} + \gamma_e B_z + \frac{\gamma_e^2 B_\perp^2}{2(\Delta_{ZFS} + \gamma_e B_z)} + \frac{\Delta_{ZFS}\gamma_e^2 B_\perp^2}{\Delta_{ZFS}^2 - \gamma_e^2 B_z^2} \\ \omega'_- &= E_3^0 + E_3^2 - (E_2^0 + E_2^2) \\ &= \Delta_{ZFS} - \gamma_e B_z + \frac{\gamma_e^2 B_\perp^2}{2(\Delta_{ZFS} - \gamma_e B_z)} + \frac{\Delta_{ZFS}\gamma_e^2 B_\perp^2}{\Delta_{ZFS}^2 - \gamma_e^2 B_z^2}. \end{aligned} \tag{34}$$

These results are shown in figure 5 as functions of $B_\perp$, where below, $e(B_\perp)$, the difference between the approximations $f = \frac{\omega'_\pm}{2\pi}$ and the exact values are plotted. Since the expressions are quadratic equations in $B_\perp$, the plots are two parabolic functions.

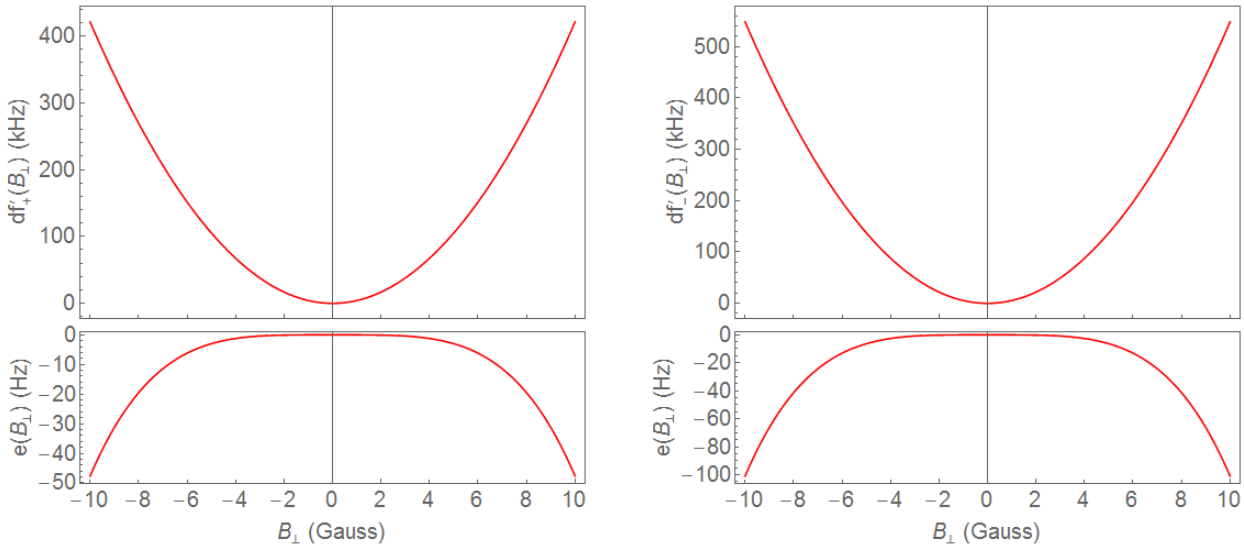

(a) Increase in frequency difference for electron spin transition $m_s = 0 \rightarrow +1$.

(b) Increase in frequency difference for electron spin transition $m_s = 0 \rightarrow -1$.

Figure 5: Approximations using second order perturbation theory of the frequency differences for electron spin transitions $m_s = 0 \rightarrow +1$ (a) and $m_s = 0 \rightarrow -1$ (b) plotted as functions of $B_\perp$. Both show parabolic behaviour, where their magnitudes increase for increasing $B_\perp$ in case of $\gamma_e B_z < \Delta_{ZFS}$. In the bottom graphs, $e(B_\perp)$ is plotted for each $f_\pm(B_\perp)$.

It is clear that the approximations are very close to the exact solutions for small $B_\perp$, since $f_\pm$ are in the order of GHz and the error is in the order of 10 Hz. As $B_\perp$ grows bigger, the difference between the approximations and exact solutions grow seemingly exponentially larger. This is because as $B_\perp$ increases, the change in eigenvalues of $\mathcal{H}$ cannot be treated as a small perturbation to the calculation of its eigenvalues anymore, and a higher order perturbation theory might be preferred. For ω_-, the error of the approximation grows larger than for ω_+. This is due to the difference of the unperturbed eigenvalues of $\mathcal{H}$ for $m_s = 0$ and $m_s = -1$ being smaller in comparison to the eigenvalues difference corresponding to $m_s = 0$ and $m_s = +1$, so the correction to the energy of the spin transition $m_s = 0 \rightarrow -1$ caused by $B_\perp$ is larger. Now if we were to take $\gamma_e B_z$ close to Δ_{ZFS}, The corrective terms E_1^2 and E_2^2 as in equations 32 will become very large, and the corrective terms of the approximations in equation 34 caused by $B_\perp$ will become very large.

Comparing $e(B_\perp)$ in figures 4 and 5, we see that for $\gamma_e B_z < \Delta_{ZFS}$ the approximations are already larger than the exact solutions, so if we were to take $\gamma_e B_z$ close to Δ_{ZFS}, the approximations would grow even larger in comparison to the exact solutions since the denominators in the fractions of equations 34 will become smaller. Looking back at equation 17, if we were to take $\gamma_e B_z$ close to Δ_{ZFS}, the energies belonging to $m_s = 0$ and $m_s = -1$ would be very close to each other, and the system may be better described as degenerate. Therefore, it may be necessary to use degenerate perturbation theory instead. However, in experiments we generally avoid the parameter regime where $\gamma_e B_z \approx \Delta_{ZFS}$, so the use of non-degenerate pertrubation theory here is justified.
With equations 34 we can find approximations for both B_z and $B_\perp$, shown in equations 35-36. To stay consistent, we have that $\omega'_- < \omega'_+$, so $B'_z > 0$. $B'_\perp$ can be either positive or negative.

$$B'_z = \frac{3\Delta_{ZFS}(\omega'_+ - \omega'_-)}{\gamma(\omega'_+ + \omega'_- - 8\Delta_{ZFS})} \tag{35}$$

$$B'_\perp = \pm\frac{2\sqrt{\Delta_{ZFS}(2\omega'_+ - \omega'_- - 4\Delta_{ZFS})(2\Delta_{ZFS} - \omega'_+ - \omega'_-)(4\Delta_{ZFS} + \omega'_+ - 2\omega'_+)}}{\gamma\sqrt{3}\sqrt{(-8\Delta_{ZFS} + \omega'_+ + \omega'_-)^2}} \tag{36}$$

4.3 Magnetic field alignment

Setting $B_\perp = 0$ would allow us to find Δ_{ZFS} and $\gamma_e B_z$ using equations 18 and 19. Therefore, we align the field such that $B_\perp = 0$.
The calibration of the magnetic field in practice is done by measuring the average of the energy differences and changing the magnetic field such that this average is at its minimum. An example of calibration in practice is shown in figure 6. We now want to know if using this method indeed corresponds to a magnetic field that is perfectly aligned, i.e. $B_\perp = 0$.

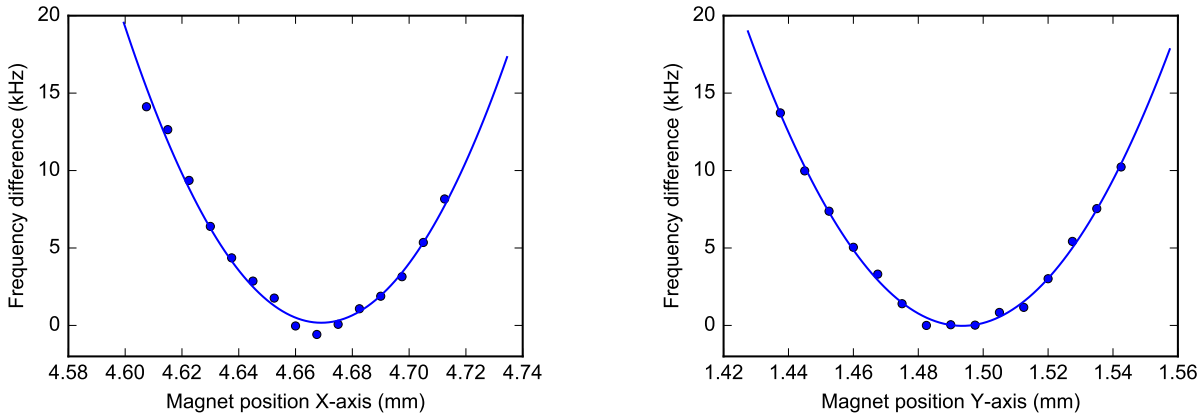

Figure 6: The frequency difference is measured for different (x, y) positions of a permanent magnet [5]. We want to confirm that the magnetic field perpendicular to the spin-direction is zero if the magnet is positioned such that the frequency difference is minimized.

Taking the derivative of the analytic average $\bar{\omega}$ with respect to $B_\perp$, shows that its derivative is zero for $B_\perp = 0$. This means that the average is at either a minimum or a maximum. For our parameter regime where $0 < \gamma_e B_z < \Delta_{ZFS}$, this results in a minimum. See Appendix A for the derivation.

From equations 34 we can also find the average of the energies, shown in equation 37. As in figure 4, the energy differences are at their minimum for $B_\perp = 0$ when using the values for the other parameters as in Appendix C where $\gamma_e B_z < \Delta_{ZFS}$, therefore the minimum of the approximated average $\bar{\omega}'$ as in equation 37 is also at its minimum.

$$\bar{\omega}' = \Delta_{ZFS} + B_\perp^2 \frac{3\gamma_e^2 \Delta_{ZFS}}{2(\Delta_{ZFS}^2 - B_z^2 \gamma_e^2)} \tag{37}$$

Indeed, for this simple system the method of calibration seems justified. However, in reality we have to take many other factors in consideration that are not included in this simplified model. In the next sections, we will have a look at more complicated models to see if this method can still be applied.

5 System with added strain

In section 4 we have neglected the strain on the crystal. Now we will see how taking this strain in consideration will affect our Hamiltonian and how the strain influences the accuracy of our approximations of its eigenvalues. Then there will also be an attempt to extract expressions for the strain using these approximations.

5.1 Using second order perturbation theory on system with added strain

The strain will be denoted as $(\epsilon_x, \epsilon_y, \epsilon_z)$. This time, we treat the terms of the Hamiltonian containing the strain and our unwanted (small valued) magnetic fields B_x and B_y as a perturbation. Unlike as in section 4, we cannot take an arbitrary coordinate system consisting of just a $\hat{\mathbf{z}}$ and $\hat{\mathbf{x}}$ direction due to the strain. Therefore we have to fix our coordinate system and also include the operator $\hat{\mathbf{S}}_y$ (equation 40). The resulting Hamiltonian $\mathcal{H}$ is shown in equations 38-39. In comparison with the matrix in equation 15, the matrix including the strain has more non-zero off-diagonal terms. Finding the eigenvalues analytically would be even more time consuming, as we have seen that even when neglecting the strain, the expressions for these eigenvalues are already large and complicated.

$$\mathcal{H} = (\Delta_{ZFS} + \epsilon_z)\hat{\mathbf{S}}_z^2 + \gamma_e(B_z\hat{\mathbf{S}}_z + B_x\hat{\mathbf{S}}_x + B_y\hat{\mathbf{S}}_y) + \epsilon_x(\hat{\mathbf{S}}_x^2 - \hat{\mathbf{S}}_y^2) + \epsilon_y(\hat{\mathbf{S}}_x\hat{\mathbf{S}}_y + \hat{\mathbf{S}}_y\hat{\mathbf{S}}_x) \tag{38}$$

$$= \begin{bmatrix} \Delta_{ZFS} + \epsilon_z + \gamma_e B_z & \frac{\gamma_e(B_x - iB_y)}{\sqrt{2}} & \epsilon_x - i\epsilon_y \\ \frac{\gamma_e(B_x + iB_y)}{\sqrt{2}} & 0 & \frac{\gamma_e(B_x - iB_y)}{\sqrt{2}} \\ \epsilon_x + i\epsilon_y & \frac{\gamma_e(B_x + iB_y)}{\sqrt{2}} & \Delta_{ZFS} + \epsilon_z - \gamma_e B_z \end{bmatrix} \tag{39}$$

$$\hat{\mathbf{S}}_y = \frac{1}{\sqrt{2}} \begin{bmatrix} 0 & -i & 0 \\ i & 0 & -i \\ 0 & i & 0 \end{bmatrix} \tag{40}$$

Instead of finding analytic expressions for the eigenvalue differences, it is more efficient to find approximations using perturbation theory. These will then be compared to the exact values of the eigenvalue differences for varying B_x and B_y, and (ϵ_x, ϵ_y) using values for the other parameters as in Appendix C.

To find the approximations, as in section 4, we start by splitting up the Hamiltonian such that $\mathcal{H} = \mathcal{H}_0 + \mathcal{H}'$ where $\mathcal{H}_0 = \mathcal{H}((B_x, B_y) = (0, 0))$ with the strain set to zero. $\mathcal{H}_0$ and $\mathcal{H}'$ are given in equations 41 and 42. Again $\mathcal{H}_0$ is a diagonal matrix from which we can read the eigenvalues.

$$\mathcal{H}_0 = (\Delta_{ZFS} + \epsilon_z)\hat{\mathbf{S}}_z^2 + \gamma_e B_z\hat{\mathbf{S}}_z \tag{41}$$

$$\mathcal{H}' = \gamma_e(B_x\hat{\mathbf{S}}_x + B_y\hat{\mathbf{S}}_y) + \epsilon_x(\hat{\mathbf{S}}_x^2 - \hat{\mathbf{S}}_y^2) + \epsilon_y(\hat{\mathbf{S}}_x\hat{\mathbf{S}}_y + \hat{\mathbf{S}}_y\hat{\mathbf{S}}_x) \tag{42}$$

Analogous to the method in section 4, ω'_+ and ω'_- are calculated and the resulting expressions are as in equations 43. By setting the strain $(\epsilon_z, \epsilon_x, \epsilon_y) = (0, 0, 0)$ and taking either $B_x = 0$ or $B_y = 0$, we get the same results as in section 4 as expected.

$$\begin{aligned} \omega'_+ &= \Delta_{ZFS} + \epsilon_z + B_z\gamma_e + \gamma_e^2(B_x^2 + B_y^2)\frac{3(\Delta_{ZFS} + \epsilon_z) - B_z\gamma_e)}{2((\Delta_{ZFS} + \epsilon_z)^2 - B_z^2\gamma_e^2)} + \frac{\epsilon_x^2 + \epsilon_y^2}{2B_z\gamma_e} \\ \omega'_- &= \Delta_{ZFS} + \epsilon_z - B_z\gamma_e + \gamma_e^2(B_x^2 + B_y^2)\frac{3(\Delta_{ZFS} + \epsilon_z) + B_z\gamma_e)}{2((\Delta_{ZFS} + \epsilon_z)^2 - B_z^2\gamma_e^2)} - \frac{\epsilon_x^2 + \epsilon_y^2}{2B_z\gamma_e}. \end{aligned} \tag{43}$$

Note that with this added strain, Δ_{ZFS} has been shifted by ϵ_z, so estimating Δ_{ZFS} is impossible if only ω_+ and ω_- are known and ϵ_z is unknown.
As equations 43 do not depend on the $\hat{\mathbf{x}}$ and $\hat{\mathbf{y}}$ components of the magnetic field and the strain, for simplification let us write $B_\perp^2 = B_x^2 + B_y^2$, which is the magnitude of the magnetic field perpendicular to $\hat{\mathbf{z}}$, and $\epsilon_\perp^2 = \epsilon_x^2 + \epsilon_y^2$, the strain perpendicular to $\hat{\mathbf{z}}$.
ω'_+ and ω'_- as in equations 43 are quadratic in $\epsilon_\perp$. The increase of the frequencies are plotted in figure 7. From these equations we can also conclude that the change of magnitude of these functions for varying $\epsilon_\perp$ are independent of $B_\perp$.

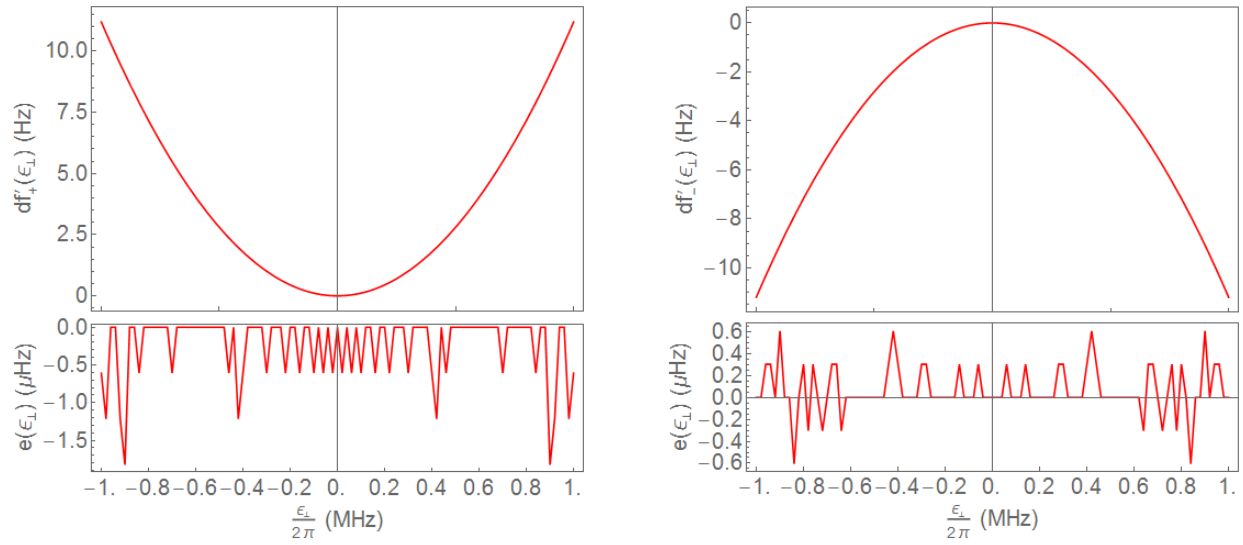

(a) Increase in frequency difference for electron spin transition $m_s = 0 \to +1$.

(b) Increase in frequency difference for electron spin transition $m_s = 0 \to -1$.

Figure 7: Frequency differences for electron spin transitions $m_s = 0 \to +1$ (a) and $m_s = 0 \to -1$ (b) as functions of $\epsilon_\perp$. Here, the influence of $B_\perp$ was neglected and thus set to zero. Notice how ω'_+ increases and ω'_- decreases for larger $\epsilon_\perp$. This means the difference in magnitude of the energy levels of the excited spin states increases. $e(B_\perp)$ is plotted below each graph for $f_\pm(B_\perp)$. This difference is very small as $f_\pm$ are in GHz. Note that neither $e(B_\perp)$ are smooth curves. This is due to the way the exact frequencies are calculated, as they are calculated using a discrete interval for $\epsilon_\perp$.

From now on, let $\Delta_Z = \Delta_{ZFS} + \epsilon_z$, the zero field splitting that has increased by ϵ_z. Then the perturbations that influence ω'_+ and ω'_- are only caused by $B_\perp$ and $\epsilon_\perp$. ω_+ and ω_- are plotted in figure 8 as functions of $B_\perp$. The strain is set to $(\epsilon_x, \epsilon_y, \epsilon_z) = (400, 400, 10)$ kHz. The other parameters have values as shown in the Appendix, with $\gamma_e B_z < \Delta_{ZFS}$. The magnitude of these functions are minimal at $B_\perp = 0$.

The difference between the exact and approximated energy differences $e(B_\perp)$ are also shown in figure 8. In comparison with $e(B_\perp)$ in figure 5, the difference between the approximations the exact solutions are larger, where especially for ω'_- the error near the region of $B_\perp = \pm 10$ Gauss has doubled.

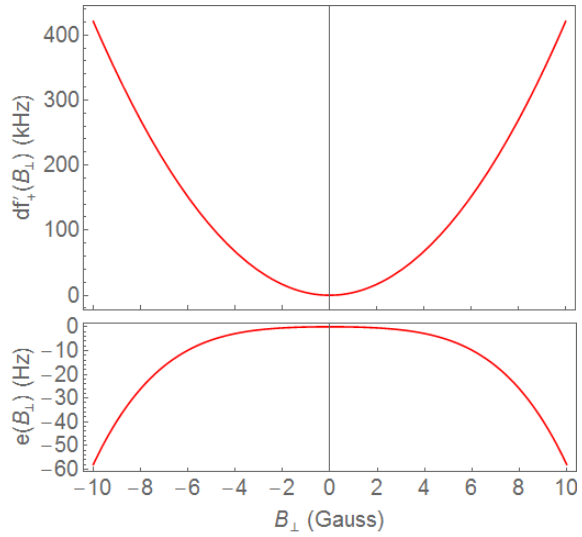

(a) Increase in frequency difference for electron spin transition $m_s = 0 \to +1$.

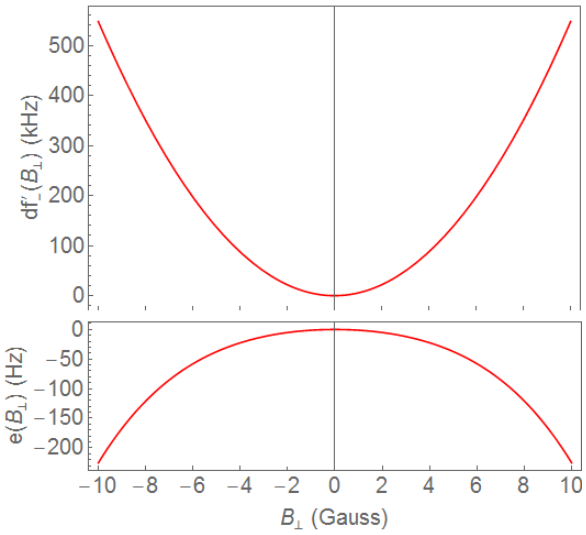

(b) Increase in frequency difference for electron spin transition $m_s = 0 \to -1$.

Figure 8: Frequency differences for electron spin transitions $m_s = 0 \to +1$ (a) and $m_s = 0 \to -1$ (b) as functions of $B_\perp$. Comparing the approximated expressions $f'_+ = \frac{\omega'_+}{2\pi}$ (a) and $f_- = \frac{\omega'_-}{2\pi}$ (b) with their respective exact solutions shows there is an increased $e(B_\perp)$ for larger $B_\perp$. As $B_\perp$ grows larger, the approximation becomes less accurate and the approximations become larger than their exact values. Both top plots are near identical to the ones in figure 5, but both $e(B_\perp)$ have increased.

From the expressions for ω'_+ and ω'_-, we can also extract approximations for B_z and $B_\perp$. These are given by equations 44-45. Taking the square root from both sides of both expressions results in a positive or negative solution. For B_z we take the positive solution, since we have assumed that $\omega_- < \omega_+$. For $B_\perp$, its sign can be either positive or negative.

$$B'^2_z = \frac{(-3(\omega'_+ - \omega'_-)\Delta_Z + \sqrt{3\Delta_Z}\sqrt{4(\omega'_+ + \omega'_-)\epsilon_\perp^2 + 3\Delta_Z((\omega'_+ - \omega'_-)^2 - 32\epsilon_\perp^2)})^2}{4\gamma_e^2(\omega'_+ + \omega'_- - 8\Delta_Z)^2} \tag{44}$$

$$\begin{aligned} B'^2_\perp = \frac{2\Delta_Z - \omega'_+ - \omega'_-}{6\gamma_e^2(\omega'_+ + \omega'_- - 8\Delta_Z)^2}\Big(&- 3\sqrt{3\Delta_Z}(\omega'_+ - \omega'_-)\sqrt{4(\omega'_+ + \omega'_-)\epsilon_\perp^2 + \Delta_Z(3(\omega'_+ - \omega'_-)^2 - 32\epsilon_\perp^2)})^2 \\ &+ 32(\omega'_+ + \omega'_-)\Delta_Z^2 - 128\Delta_Z^3 + 6(\omega'_+ + \omega'_-)\epsilon_\perp^2 + \Delta_Z(7\omega'^2_+ - 22\omega'_+\omega'_- + 7\omega'^2_- - 48\epsilon_\perp^2)\Big) \end{aligned} \tag{45}$$

Finding expressions for ϵ_x, ϵ_y and ϵ_z in terms of known parameters is not possible from equations 43, even if we were to set $B_\perp = 0$. In section 4, there were three parameters (counting $\gamma_e B_z$ as one) and two equations of which it was experimentally possible to find all parameters. But now there are three more parameters introduced, $(\epsilon_x, \epsilon_y, \epsilon_z)$, which makes it impossible to find expressions for the parameters independent of each other anymore. Therefore it is not possible to find values for the strain with equations 43 using just the method of second order perturbation theory.

5.2 Magnetic Field Alignment

If $B_\perp = 0$, and the strain neglected, we get the same situation as in the previous section. We want to see if the method of alignment is still valid if the strain is included in the model.
The approximated average energy difference $\bar{\omega}'$ is given in equation 46, which is a quadratic function in $B_\perp$. Indeed, this is very similar to equation 37.

$$\bar{\omega}' = \frac{\omega'_+ + \omega'_-}{2} = \Delta_Z + B_\perp^2 \frac{3\gamma_e^2 \Delta_Z}{2(\Delta_Z^2 - B_z^2\gamma_e^2)} \tag{46}$$

We can then conclude that its minimum is at $B_\perp = 0$ for our parameter regime as shown in the Appendix, since $\bar{\omega}'$ is a quadratic function of $B_\perp$ and $\gamma_e B_z < \Delta_{ZFS} + \epsilon_z$. This can also be concluded by looking at figure 8 where both ω'_+ and ω'_- are minimal at $B_\perp = 0$. Therefore, including the strain in the model did not show that the current method of calibrating the magnetic field is invalid.

6 System with added nitrogen nuclear spin

In the previous two sections, we have only considered the electron spin. However, the nitrogen atom in the NV center has a nuclear spin-1 which also affects the energy levels of the electron. This spin causes the energy levels to split as shown in figure 9, and the dimensions Hamiltonian of this system will be three times larger and more complicated due to off-diagonal terms as we will see. Expressing eigenvalues of the resulting matrix would be very difficult to do analytically, therefore we will have to rely on perturbation theory. After finding these approximations for the eigenvalues, the results will be compared to yet another exact case for a specific set of values (see Appendix C). It will be interesting to compare the error with the previous sections, to see how good of an approximation perturbation theory gives for a larger and much more complicated system.

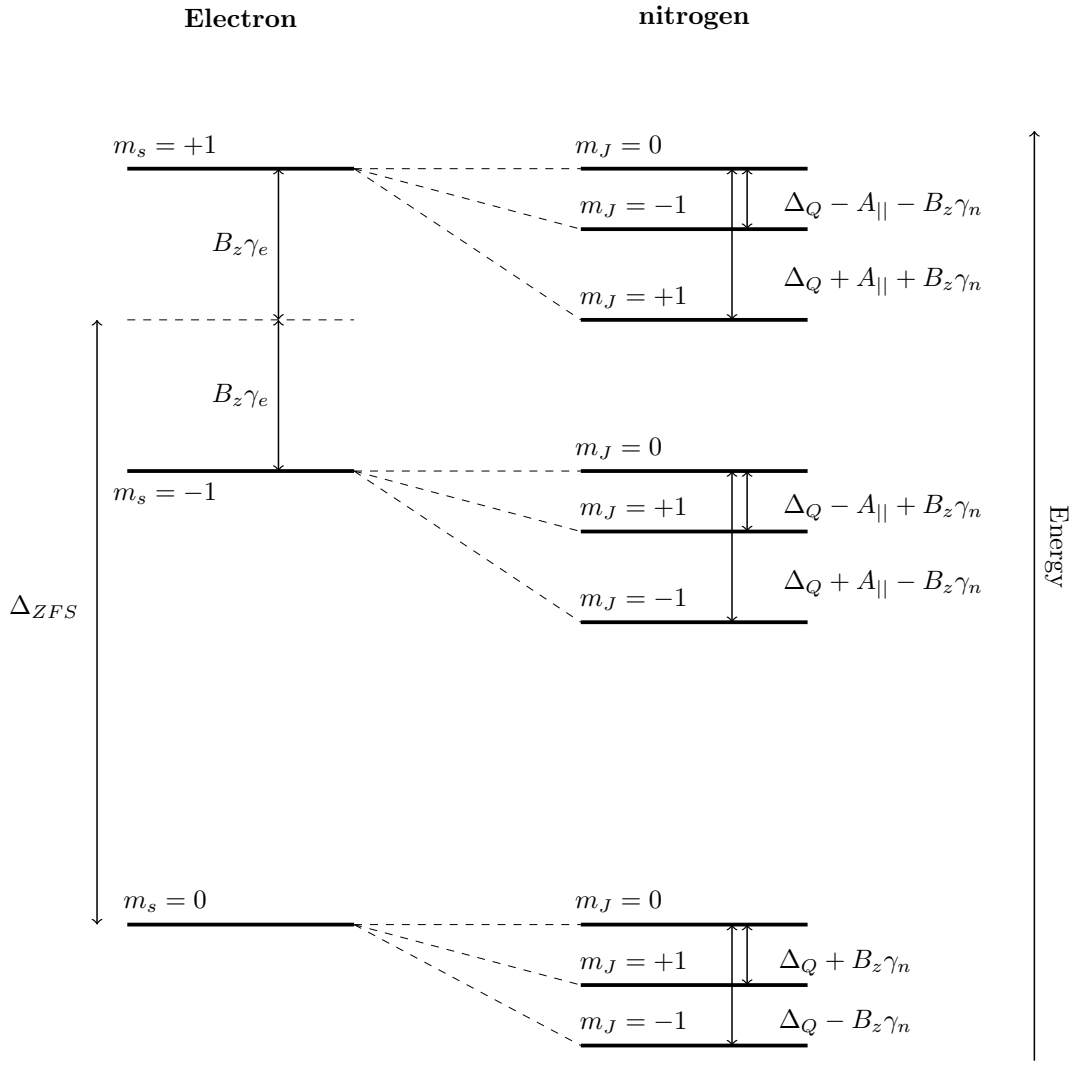

Figure 9: Splitting of the energy levels of the electron due to the nitrogen spin in absence of the magnetic field (B_x, B_y) perpendicular to $\hat{\mathbf{z}}$, strain and the perpendicular hyperfine coupling $A_\perp$.

6.1 Finding the energy differences with added nitrogen nuclear spin

Let us consider the system as described in section 5, where we now take the nuclear spin of the nitrogen atom into account. Just like the electron, the nitrogen nuclear spin has three energy levels for spin states $m_J = -1, 0, 1$. For the joint system, there are thus a total of nine possible states $|m_s, m_J\rangle$. The Hamiltonian will therefore be a 9×9 matrix, given by equation 47, where $\mathcal{H}_e$, $\mathcal{H}_n$ and $\mathcal{H}_{hf}$ are given by equations 48-50 [1] [7].

$$\mathcal{H} = \mathcal{H}_e + \mathcal{H}_n + \mathcal{H}_{hf} \tag{47}$$

$$\mathcal{H}_e = (\Delta_{ZFS} + \epsilon_z)\hat{\mathbf{S}}_z^2 + \gamma_e(B_x\hat{\mathbf{S}}_x + B_y\hat{\mathbf{S}}_y + B_z\hat{\mathbf{S}}_z) + \epsilon_x(\hat{\mathbf{S}}_x^2 - \hat{\mathbf{S}}_y^2) + \epsilon_y(\hat{\mathbf{S}}_x\hat{\mathbf{S}}_y + \hat{\mathbf{S}}_y\hat{\mathbf{S}}_x) \tag{48}$$

$$\mathcal{H}_n = \Delta_Q\hat{\mathbf{J}}_z^2 + \gamma_n(B_x\hat{\mathbf{J}}_x + B_y\hat{\mathbf{J}}_y + B_z\hat{\mathbf{J}}_z) \tag{49}$$

$$\mathcal{H}_{hf} = A_\perp(\hat{\mathbf{S}}_x\hat{\mathbf{J}}_x + \hat{\mathbf{S}}_y\hat{\mathbf{J}}_y) + A_\parallel(\hat{\mathbf{S}}_z\hat{\mathbf{J}}_z) \tag{50}$$

There are now also a few more parameters to consider in these equations. Δ_Q is the quadrupole splitting of the nitrogen atom, γ_n is the nitrogen gyromagnetic ratio and $\hat{\mathbf{J}}_x, \hat{\mathbf{J}}_y, \hat{\mathbf{J}}_z$ are the same spin matrices as $\hat{\mathbf{S}}_x$, $\hat{\mathbf{S}}_y$ and $\hat{\mathbf{S}}_z$. $A_\parallel$ and $A_\perp$ are the hyperfine coupling between the electron spin and nitrogen nuclear spin, where $A_\parallel$ is along the $\hat{\mathbf{z}}$ direction and $A_\perp$ is perpendicular to $\hat{\mathbf{z}}$.

Writing $\mathcal{H}$ as a matrix shows that there are now many off-diagonal terms which makes analytically calculating the eigenvalues of this 9×9 matrix very difficult. Instead of attempting to do this, we will be estimating the eigenvalues of this matrix using perturbation theory, where again we treat the magnetic field perpendicular to $\hat{\mathbf{z}}$, (B_x, B_y), the strain, and now also the perpendicular hyperfine coupling $A_\perp$ as the perturbation.

Synonymous to the methods of sections 4 and 5, we start by writing $\mathcal{H} = \mathcal{H}_0 + \mathcal{H}'$, where $\mathcal{H}_0$ and $\mathcal{H}'$ are given by equations 51-52.

$$\mathcal{H}_0 = (\Delta_{ZFS} + \epsilon_z)\hat{\mathbf{S}}_z^2 + \gamma_e B_z\hat{\mathbf{S}}_z + \Delta_Q\hat{\mathbf{J}}_z^2 + \gamma_n B_z\hat{\mathbf{J}}_z + A_\parallel\hat{\mathbf{S}}_z\hat{\mathbf{J}}_z \tag{51}$$

$$\begin{aligned}\mathcal{H}' =& \gamma_e(B_x\hat{\mathbf{S}}_x + B_y\hat{\mathbf{S}}_y) + \epsilon_x(\hat{\mathbf{S}}_x^2 - \hat{\mathbf{S}}_y^2) + \epsilon_y(\hat{\mathbf{S}}_x\hat{\mathbf{S}}_y + \hat{\mathbf{S}}_y\hat{\mathbf{S}}_x) \\ &+ \gamma_n(B_x\hat{\mathbf{J}}_x + B_y\hat{\mathbf{J}}_y) + A_\perp(\hat{\mathbf{S}}_x\hat{\mathbf{J}}_x + \hat{\mathbf{S}}_y\hat{\mathbf{J}}_y)\end{aligned} \tag{52}$$

The energy differences of the spin states will be denoted as $\omega_{e\pm}^k$ for fixed $m_J = k$ and measuring energy transition $m_s = 0 \to \pm 1$, and $\omega_{n\pm}^k$ for fixed $m_s = k$ and measuring energy transition $m_J = 0 \to \pm 1$. Note that the energy differences of belonging to $m_s = \mp 1 \to \pm 1$ and $m_J = \mp 1 \to \pm 1$ cannot easily be measured in practice. If it were possible, then it would not give any new information on the energy levels anyway.

The approximated eigenvalues of $\mathcal{H}$ obtained with second order perturbation theory are shown in appendix D and the eigenvalue differences are shown in E for both the electron spin transitions and the nitrogen nuclear spin transitions.

The frequency differences for all electron spin transitions are shown in figure 10. The increase of frequencies for different $B_\perp$ were nearly identical, therefore only the frequency differences themselves are shown.

[1] Note that there are implied tensor products between all operators. For operators $\hat{\mathbf{S}}_i$ and $\hat{\mathbf{J}}_j$, $i, j = x, y, z$, we actually have $\hat{\mathbf{S}}_i \otimes I_3$, $I_3 \otimes \hat{\mathbf{J}}_j$ and $\hat{\mathbf{S}}_i\hat{\mathbf{J}}_j = \hat{\mathbf{S}}_i \otimes \hat{\mathbf{J}}_j$, where I_3 is the 3×3 identity matrix. Then we actually have $\mathcal{H} = \mathcal{H}_e \otimes I_3 + I_3 \otimes \mathcal{H}_n + \mathcal{H}_{hf}$, but we leave out all tensor products "$\otimes$" and identity matrices I_3 in equations 47-50 as a convention.

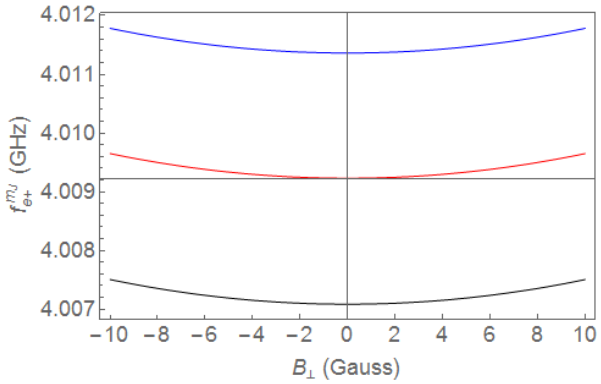

(a) f_{e+}^{-1} (blue), f_{e+}^{0} (red) and f_{e+}^{+1} (black) plotted as functions of $B_\perp$, which are the frequencies corresponding to the spin transitions $m_s = 0 \rightarrow +1$ for fixed $m_J = -1, 0, +1$.

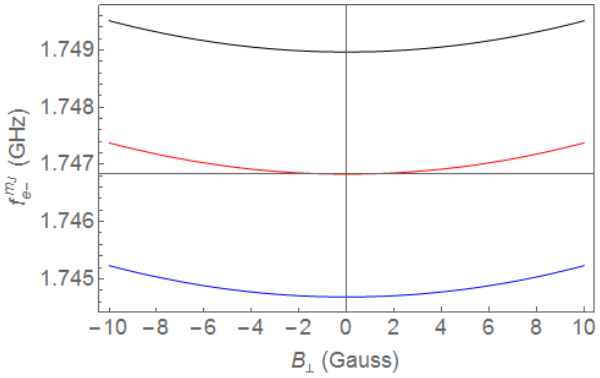

(b) f_{e-}^{-1} (blue),f_{e-}^{0} (red) and f_{e-}^{+1} (black) plotted as functions of $B_\perp$, which are the frequencies corresponding to the spin transitions $m_s = 0 \rightarrow -1$ for fixed $m_J = -1, 0, +1$.

Figure 10: The frequency differences of the spin transitions $m_s = 0 \rightarrow +1$ (a) and $m_s = 0 \rightarrow -1$ (b) for fixed nitrogen spins $m_J = -1, 0, 1$ are plotted as functions of $B_\perp$. Each plot shows parabolic behaviour, where at $B_\perp = 0$ their magnitudes are minimized.

As an example, we shall compare f_{e+}^{0} and f_{e-}^{0} with the exact solutions as these quantities are usually measured in practice. The results are shown in figure 11.

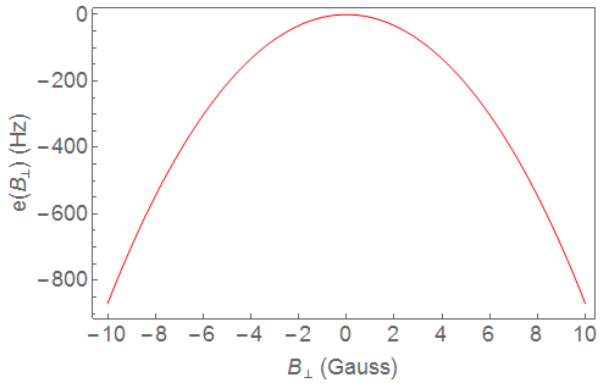

(a) $e(B_\perp)$ for electron spin transition $m_s = 0 \rightarrow +1$.

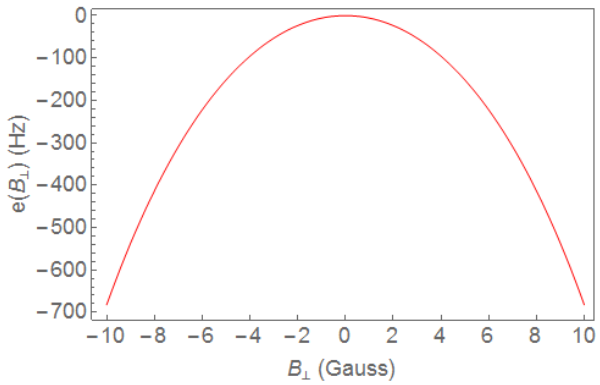

(b) $e(B_\perp)$ for electron spin transition $m_s = 0 \rightarrow -1$.

Figure 11: The error of the estimations $e(B_\perp)$ for f_{e+}^{0} (a) and f_{e-}^{0} (b) compared to their respective exact solutions are plotted as functions of $B_\perp$. Both $f_{e\pm}^{0}$ grow larger than their exact values as $B_\perp$ increases. Note how the error has increased nearly ten-fold compared to estimations in figures 5 and 8, where the influence of the nuclear spin of the nitrogen atom in the models was not included. This increase in $e(B_\perp)$ is due to the perpendicular hyperfine coupling $A_\perp$ in equation 47.

Compared to the previous findings in figures 5 and 8, the error now has increased by a significant amount, as it is now in hundreds of Hz. Interesting is how now the difference between the approximation and the exact value of f_{e-}^{0} seems to be smaller than f_{e+}^{0} which was not the case in the previous sections. The increase in $e(B_\perp)$ for the frequency differences of both spin transitions is due to the perpendicular hyperfine coupling $A_\perp$. This is further explored in figure 12.

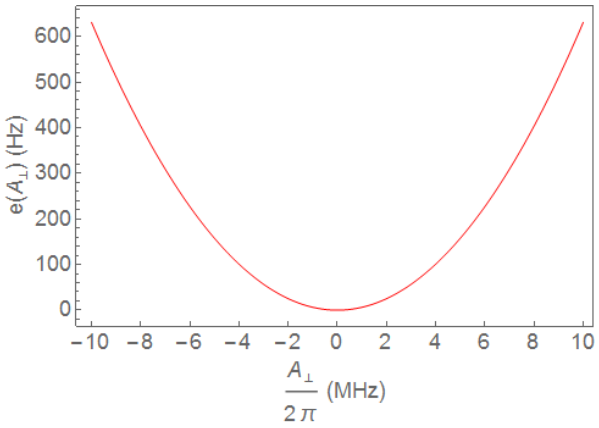

(a) $e(A_\perp)$ for electron spin transition $m_s = 0 \to +1$.

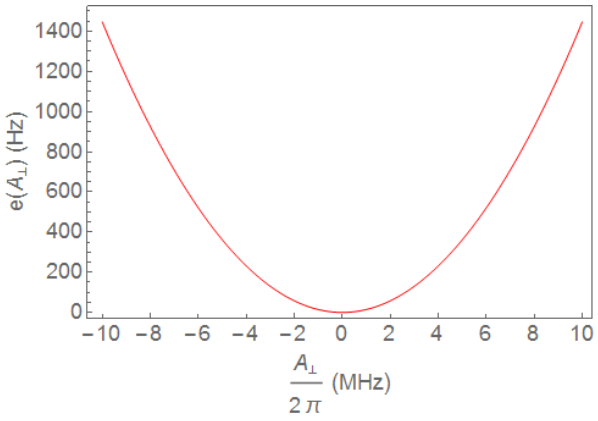

(b) $e(A_\perp)$ for electron spin transition $m_s = 0 \to -1$.

Figure 12: The error of the estimations $e(A_\perp)$ for f^0_{e+} (a) and f^0_{e-} (b) compared to their respective exact solutions are plotted as functions of $A_\perp$. In these plots, $B_\perp = 0$. Both $f^0_{e\pm}$ grow larger than their exact values as $A_\perp$ increases. The error becomes very large for larger $A_\perp$. In practice, $A_\perp$ is fairly well known and about -2.7 MHz [7].

Indeed, for increasing $A_\perp$, the difference between the exact values and the approximated values for $f^0_{e\pm}$ increases significantly.

6.2 Magnetic Field Alignment

Let us assume $m_J = 0$ as an example. Using second order perturbation theory, the average $\bar{\omega}$ is a quadratic function in $B_\perp$ and can be written as in equation 53, where the functions F and G are independent of $B_\perp$, used to simplify the analysis of $\bar{\omega}$. The full expression can be found in Appendix B.

$$\bar{\omega} = B_\perp^2 F + G \tag{53}$$

Taking the derivative with respect to $B_\perp$ gives $\dfrac{\delta\bar{\omega}}{\delta B_\perp} = 2B_\perp F$, so its derivative is zero at $B_\perp = 0$. Then using the parameters as in Appendix C where $\gamma_e B_z < \Delta_{ZFS} + \epsilon_z$, $\bar{\omega}$ is minimal for $B_\perp = 0$. This can also be confirmed by looking at figure 10, where ω^0_{e+} and ω^0_{e-} are at their minimum at $B_\perp = 0$.

Just as in the simplified models in sections 4 and 5, the method of magnetic field calibration has not been proven to be incorrect if the influence nuclear spin of the nitrogen atom is also considered.

6.3 Estimating the quadrupole splitting

Using the approximations of the measurable frequencies, an estimate for the quadrupole splitting Δ_Q can be found. Looking at the averages of the measurable frequency differences due to the nitrogen nuclear spin transitions for different spins of the electron, there are a few options for the estimate. These are plotted as functions of Δ_Q in figure 13. The perpendicular magnetic field $B_\perp$ and the strain are neglected.

From these expressions, there might be a better estimate. Looking at figure 13, it seems that averaging all the average frequency differences of all the nitrogen nuclear spin transitions for all electron spin states may be a better approximation. The average of all nitrogen nuclear spin transitions for all electron spins is

given by the approximation

$$\begin{aligned}\sum_{i=-1}^{+1}(\omega_{n+}^{i}+\omega_{n-}^{i}) =&6\Delta_Q+3A_\perp^2\left(\frac{1}{-A_\parallel+B_z(\gamma_e-\gamma_n)+\Delta_Q+\Delta_Z}+\frac{1}{-A_\parallel+B_z(\gamma_n-\gamma_e)+\Delta_Q+\Delta_Z}\right)\\&+3A_\perp^2\left(\frac{1}{B_z(\gamma_n-\gamma_e)+\Delta_Q-\Delta_Z}+\frac{1}{B_z(\gamma_e-\gamma_n)+\Delta_Q-\Delta_Z}\right),\\=&6\Delta_Q+3A_\perp^2\left(\frac{2(\Delta_Q+\Delta_Z-A_\parallel)}{(\Delta_Q+\Delta_Z-A_\parallel)^2-B_z^2(\gamma_e-\gamma_n)^2}+\frac{2(\Delta_Q-\Delta_Z)}{(\Delta_Q-\Delta_Z)^2-B_z^2(\gamma_e-\gamma_n)^2}\right).\end{aligned} \tag{54}$$

Since Δ_Q and $A_\parallel$ are very small compared to Δ_Z, the second term containing all the fractions is very small as well. To see how well of an approximation this is, it is plotted in figure 13 along with the averages for each electron spin separately as functions of $A_\perp$.

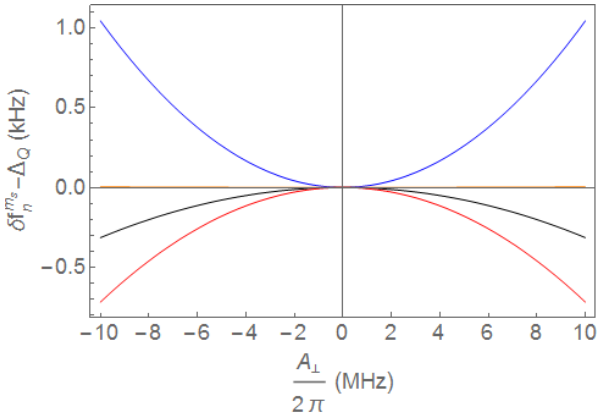

(a) Accuracy of the estimation of Δ_Q for the average of frequency difference for nitrogen spin transitions for different electron spins ($m_s=+1$ (black), $m_s=0$ (blue) and $m_s=-1$ (red)) as functions of $A_\perp$. The average of all three frequency difference average for the nitrogen spin transitions is plotted in orange.

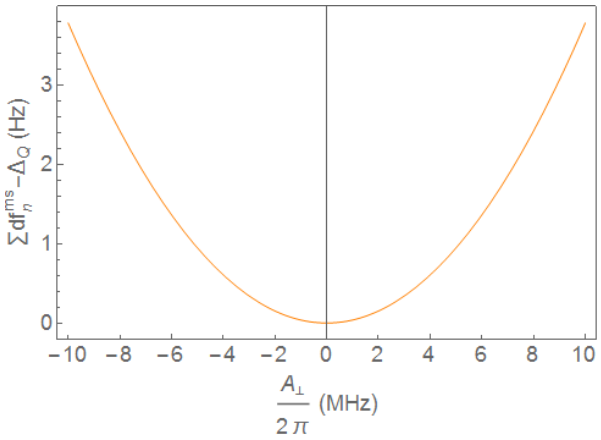

(b) Accuracy of the estimation of Δ_Q for the average of all frequency differences for the nitrogen spin transitions for all electron spins as function of $A_\perp$.

Figure 13: In figure (a), the differences average of all frequency differences for the nitrogen nuclear spin transitions for each electron spin states and the quadrupole splitting are plotted along with the difference between the frequency difference of all nitrogen nuclear spins for all electron spin states with the quadrupole splitting. As the orange curve is difficult to see in (a), it is again plotted in (b). In figure (b), the second term of equation 54 is plotted as a function of $A_\perp$ (divided by 6). Note how the difference between the average of all nitrogen nuclear spin transitions for all electron spin states and the quadrupole splitting us in the order of a few Hz for our parameter regime, while the difference between the average of all nitrogen nuclear spin transitions for each electron state separately and the quadrupole splitting is in the order of kHz.

Indeed for increasing $A_\perp$, the average of all nitrogen nuclear spin transitions for all electron spins is a better estimate for the quadrupole splitting.

Neglecting the second term in equation 54 already results in a fairly good approximation for Δ_Q. Then the error on the estimate is only a result of the accuracy of the measurements, which are in the order of 0.1 Hz. Due to the propagation of error, the resulting error on Δ_Q is only a few Hz. In practice, there are already good estimates for $A_\parallel$ and $A_\perp$, and if there were estimates for Δ_Z and B_z, equation 54 could perhaps be fully solved for Δ_Q and possibly be a better approximation.
These estimates for Δ_Z and $B_z\gamma_e$ can be made by using the same method as in section 4, where the strain is neglected and the average and difference of the electron spin transitions are found for $m_J=0$ (see figure 9).

To then attempt to find a better approximation for Δ_Q, we first approximate Δ_Q in the simplest way.

$$\widetilde{\Delta}_Q = \frac{1}{6}\left(\sum_{i=-1}^{+1}(\omega_{n+}^i + \omega_{n-}^i)\right) \tag{55}$$

Then the second approximation will be made by substituting $\widetilde{\Delta}_Q$ in the second term of equation 54. Since that term does not change much for different $\widetilde{\Delta}_Q$ in our parameter regime, this will result in a better approximation for Δ_Q.

$$\Delta_Q = \widetilde{\Delta}_Q - \frac{1}{2}A_\perp^2\left(\frac{2(\widetilde{\Delta}_Q + \Delta_Z - A_\parallel)}{(\widetilde{\Delta}_Q + \Delta_Z - A_\parallel)^2 - B_z^2(\gamma_e - \gamma_n)^2} + \frac{2(\widetilde{\Delta}_Q - \Delta_Z)}{(\widetilde{\Delta}_Q - \Delta_Z)^2 - B_z^2(\gamma_e - \gamma_n)^2}\right) \tag{56}$$

Of course now the error of Δ_Q increases due to this second term. This error is caused by the approximations made for Δ_Z and B_z, and the errors on the parameters $A_\perp$, $A_\parallel$ which are taken as 0.07 MHz for each [7]. The errors on the gyromagnetic ratios are neglected as they are very small.

Measurements for all measurable spin transitions are shown in the tables below, where $B_\perp$ is set to zero.

transition	frequency difference (kHz)
ω_{n+}^{+1}	7263.393(1)
ω_{n-}^{+1}	2636.928(1)
ω_{n+}^{0}	4823.184(1)
ω_{n-}^{0}	5069.115(1)
ω_{n+}^{-1}	2884.864(1)
ω_{n-}^{-1}	7017.226(1)

transition	frequency difference (MHz)
ω_{e+}^{+1}	4006.452(2)
ω_{e-}^{+1}	1748.841(2)
ω_{e+}^{0}	4008.648(3)
ω_{e-}^{0}	1746.663(2)
ω_{e+}^{-1}	4010.83(3)
ω_{e-}^{-1}	1744.471(3)

Using these measurements, Δ_Q can be approximated using formulas 55 and 56. Note that it is not clear whether these frequency differences are positive or negative. Therefore, for both cases Δ_Q will be calculated. First, a rough estimate for B_z and Δ_{ZFS} has to be made, and for that using the electron spin transitions for $m_J = 0$ and equations 18 and 19 result in

$$B_z \approx 0.04(1) \text{ Tesla}$$
$$\Delta_{ZFS} \approx 2.8(1) \text{ MHz}.$$

As these estimates are rough, the error were taken to be fairly large with errors $\delta(B_z) = 100$ Gauss and $\delta(\Delta_{ZFS}) = 10^8$ Hz. The first approximations for the positive and negative quadrupole splitting ($\widetilde{\Delta}_Q^+$ and $\widetilde{\Delta}_Q^-$ respectively) calculated using all nitrogen nuclear spin transitions (formula 55) is as follows:

$$\widetilde{\Delta}_Q^+ = 4949.1183(2) \text{ kHz}$$
$$\widetilde{\Delta}_Q^- = -4949.1183(2) \text{ kHz}.$$

The errors are calculated using the errors from the measurements. Then using formula 56, the second approximations for both are

$$\Delta_Q^+ = 4949.25(2) \text{ kHz}$$
$$\Delta_Q^- = -4949.11(1) \text{ kHz}.$$

Comparing Δ_Q^- to the previous finding of $\Delta_Q = -4.945 \pm 0.005$ MHz [7], the new finding is within the region of error of the previous finding.

7 Conclusion

In section 4, where only the Hamiltonian of the electron without strain was considered, it was possible to find the parameters Δ_{ZFS}, $\gamma_e B_z$ analytically only if $B_\perp = 0$. If $B_\perp \neq 0$, then we could not find expressions for all parameters in terms of known frequency measurements. In section 5 where the strain was included in the Hamiltonian, it impossible to find the individual parameters, even is $B_\perp = 0$. Still, it is possible to know if the perpendicular magnetic field $B_\perp$ is set to zero using multiple measurements. Setting $B_\perp = 0$ was also possible for the system in section 6 where the nitrogen nuclear spin was also considered. Because of the influence of the nitrogen nuclear spin there were now eight measurable eigenvalue differences of the Hamiltonian to be found, but also more parameters to be considered. Finding all the parameters has not yet been possible. However, neglecting the strain does make it possible to find estimations for the parameters $\gamma_e B_z$, Δ_{ZFS} and Δ_Q and setting $B_\perp$ to zero further simplifies the problem. We have found that the quadrupole splitting Δ_Q can be estimated using experimental data and rough estimations for the other parameters. We cannot know wether this Δ_Q is positive or negative with these measurements alone, therefore it is estimated twice, once assuming it was positive, and once assumnig it was negative. This results in the estimations $\Delta_Q^+ = 4949.25(2)$ kHz and $\Delta_Q^- = -4949.11(1)$ kHz.

Indeed, second order perturbation theory has proven it to be possible to estimate parameters in the Hamiltonian of the NV center and perhaps will be a great method to further our understanding of the NV center.

A Derivative of $\bar{\omega}$ with respect to $B_\perp$

Before simplification, the average eigenvalue difference for the Hamiltonian as described in 4, equation 15 is shown below.

$$\bar{\omega} = 2^{\frac{2}{3}} \frac{2^{\frac{2}{3}} G + H^2}{4H},$$

$$\begin{aligned} F(B_z, B_\perp) &= \Delta_{ZFS}(3^2\gamma^2(B_\perp^2 - 2B_z^2) + 2\Delta_{ZFS}^2) \\ G(B_z, B_\perp) &= 3\gamma^2(B_\perp^2 + B_z^2) + \Delta_{ZFS}^2 \\ H(F, G) &= (F + \sqrt{F^2 - 4G^3})^{\frac{1}{3}}. \end{aligned}$$

Taking the derivative with respect to $B_\perp$ results in an expression with partial derivatives of the functions G, F and H.

$$\begin{aligned} \frac{\delta\bar{\omega}}{\delta B_\perp} &= 2^{\frac{2}{3}} \left(\frac{2^{\frac{2}{3}}}{4} \frac{\delta}{\delta B_\perp} \frac{G}{H} + \frac{1}{4} \frac{\delta H}{\delta B_\perp} \right) \\ &= 2^{\frac{2}{3}} \left(\frac{2^{\frac{2}{3}}}{4} \left(\frac{1}{H} \frac{\delta G}{\delta B_\perp} + G \frac{\delta}{\delta B_\perp} \frac{1}{H} \right) + \frac{1}{4} \frac{\delta H}{\delta B_\perp} \right) \\ &= 2^{\frac{2}{3}} \left(\frac{2^{\frac{2}{3}}}{4} \left(\frac{1}{H} \frac{\delta G}{\delta B_\perp} - \frac{G}{H^2} \frac{\delta H}{\delta B_\perp} \right) + \frac{1}{4} \frac{\delta H}{\delta B_\perp} \right) \end{aligned}$$

These partial derivatives are given by

$$\begin{aligned} \frac{\delta G}{\delta B_\perp} &= 6\gamma_e^2 B_\perp, \\ \frac{\delta F}{\delta B_\perp} &= 18\Delta_{ZFS}\gamma_e^2 B_\perp, \\ \frac{\delta H}{\delta B_\perp} &= \frac{\delta}{\delta B_\perp}(F + \sqrt{F^3 - 4G^2})^{\frac{1}{3}} \\ &= \frac{1}{3(F + \sqrt{F^3 - 4G^2})^{\frac{2}{3}}} \frac{\delta}{\delta B_\perp}(F + \sqrt{F^3 - 4G^2}) \\ &= \frac{1}{3H^2} \left(\frac{\delta F}{\delta B_\perp} + \frac{\delta}{\delta B_\perp} \sqrt{F^3 - 4G^2} \right) \\ &= \frac{1}{3H^2} \left(\frac{\delta F}{\delta B_\perp} + \frac{1}{\sqrt{F^3 - 4G^2}} \left(\frac{\delta F^3}{\delta B_\perp} - 4 \frac{\delta G^2}{\delta B_\perp} \right) \right) \\ &= \frac{1}{3H^3} \left(\frac{\delta F}{\delta B_\perp} + \frac{1}{\sqrt{F^3 - 4G^2}} \left(3F^2 \frac{\delta F}{\delta B_\perp} - 8G \frac{\delta G}{\delta B_\perp} \right) \right). \end{aligned}$$

In our parameter regime $H(0) \neq 0$ and $\sqrt{F(0)^3 - 4G(0)^2} \neq 0$. Then we have that the partial derivatives of the functions G, F and H are zero for $B_\perp$.

$$\left. \frac{\delta G}{\delta B_\perp} \right|_{B_\perp = 0} = 0, \quad \left. \frac{\delta F}{\delta B_\perp} \right|_{B_\perp = 0} = 0, \quad \left. \frac{\delta H}{\delta B_\perp} \right|_{B_\perp = 0} = 0.$$

Therefore, the derivative of $\bar{\omega}$ with respect to $B_\perp$ is zero for $B_\perp = 0$.

$$\left. \frac{\delta\bar{\omega}}{\delta B_\perp} \right|_{B_\perp = 0} = 0$$

This means that $\bar{\omega}(B_\perp)$ is at its maximum or minimum. For our parameter regime, $\bar{\omega}$ is at its minimum.

B Average energy difference for $m_J = 0$

$$
\begin{aligned}
\bar{\omega} &= B_\perp^2 F + G \\
F &= \frac{\gamma_n^2 \Delta_Q}{\Delta_Q^2 - B_z^2 \gamma_n^2} - \frac{1}{2} \frac{\gamma_n^2 \left(A_z + \Delta_Q\right)}{(A_z + \Delta_Q)^2 - B_z^2 \gamma_n^2} + \frac{1}{2} \frac{\gamma_n^2 \left(A_z - \Delta_Q\right)}{(A_z - \Delta_Q)^2 - B_z^2 \gamma_n^2} + \frac{3}{2} \frac{\gamma_e^2 \left(\epsilon_z + \Delta_{\mathrm{ZFS}}\right)}{(\Delta_{\mathrm{ZFS}} + \epsilon_z)^2 - B_z^2 \gamma_e^2} \\
&= \frac{\gamma_n^2 \Delta_Q}{\Delta_Q^2 - B_z^2 \gamma_n^2} - \frac{\gamma_n^2 (A_z (A_z^2 - \Delta_Q^2) - B_z^2 \gamma_n^2 (A_z^2 + \Delta_Q^2))}{((A_z + \Delta_Q)^2 - B_z^2 \gamma_n^2)((A_z - \Delta_Q)^2 - B_z^2 \gamma_n^2)} + \frac{3}{2} \frac{\gamma_e^2 \left(\epsilon_z + \Delta_{\mathrm{ZFS}}\right)}{(\Delta_{\mathrm{ZFS}} + \epsilon_z)^2 - B_z^2 \gamma_e^2} \\
G &= \frac{2 A_x^2 \left(A_z - \Delta_Q - \epsilon_z - \Delta_{\mathrm{ZFS}}\right)}{B_z^2 (\gamma_e - \gamma_n)^2 - (A_z - \Delta_Q - \Delta_{\mathrm{ZFS}} - \epsilon_z)^2} + \frac{A_x^2 \left(\Delta_Q - \epsilon_z - \Delta_{\mathrm{ZFS}}\right)}{B_z^2 (\gamma_e - \gamma_n)^2 - (\Delta_Q - \Delta_{\mathrm{ZFS}} - \epsilon_z)^2}
\end{aligned}
$$

C Used parameters for comparisons

Parameter	Description	Estimated value	source
Δ_{ZFS}	electron zero-field splitting	2.877623 GHz	[9]
Δ_Q	nitrogen quadrupole splitting	-4.945 MHz	[7]
γ_e	electron gyromagnetic ratio	2.8031 MHz/G	[7]
γ_n	nitrogen gyromagnetic ratio	0.3077 kHz/G	[10]
B_z	magnetic field aligned to spin direction	403.553 G	[9]
$\{\epsilon_x, \epsilon_y, \epsilon_z\}$	strain	$\{400, 400, 10\}$ kHz	Estimate
$\{A_\perp, A_\parallel\}$	hyperfine coupling	$\{-2.7, -2.14\}$ MHz	[7]

D Eigenvalues of Hamiltonian including nitrogen spin.

The following eigenvalues are simplified using the following subsitutions:

$$B_\perp^2 = B_x^2 + B_y^2$$
$$\Delta_Z = \Delta_{ZFS} + \epsilon_z$$
$$\epsilon_\perp^2 = \epsilon_x^2 + \epsilon_y^2.$$

The eigenvalues are denoted as E_{m_s,m_J}, where $E_{x,y}$ is the energy level belonging to $m_s = x$ and $m_J = y$

$$\begin{aligned}
E_{+1,+1} =& \frac{B_\perp^2\gamma_e^2}{2A_\parallel + B_z\gamma_e + \Delta_Z} + B_z\gamma_e + \frac{\epsilon_\perp^2}{2A_\parallel + 2B_z\gamma_e} + A_\parallel + B_z\gamma_n + \Delta_Q + \Delta_Z \\
&+ \frac{B_\perp^2\gamma_n^2}{2A_\parallel + B_z\gamma_n + \Delta_Q} \\
E_{+1,0} =& \frac{A_\perp^2}{B_z\gamma_e - B_z\gamma_n - \Delta_Q + \Delta_Z} + \frac{\epsilon_\perp^2}{2B_z\gamma_e} + B_z\gamma_e + \Delta_Z \\
&+ \frac{B_\perp^2\gamma_n^2}{2A_\parallel + B_z\gamma_n - \Delta_Q} + \frac{B_\perp^2\gamma_n^2}{2 - A_\parallel - B_z\gamma_n - \Delta_Q} + \frac{B_\perp^2\gamma_e^2}{2B_z\gamma_e + \Delta_Z} \\
E_{+1,-1} =& \frac{A_\perp^2}{-A_\parallel + B_z\gamma_e - B_z\gamma_n + \Delta_Q + \Delta_Z} + \frac{\epsilon_\perp^2}{2B_z\gamma_e - 2A_\parallel} \\
&- A_\parallel + B_z\gamma_e - B_z\gamma_n + \Delta_Q + \Delta_Z + \frac{B_\perp^2\gamma_n^2}{2 - A_\parallel - B_z\gamma_n + \Delta_Q} + \frac{B_\perp^2\gamma_e^2}{2 - A_\parallel + B_z\gamma_e + \Delta_Z} \\
E_{0,+1} =& \frac{A_\perp^2}{-B_z\gamma_e + B_z\gamma_n + \Delta_Q - \Delta_Z} + B_z\gamma_n + \Delta_Q + \frac{B_\perp^2\gamma_n^2}{2B_z\gamma_n + \Delta_Q} + \frac{B_\perp^2\gamma_e^2}{2A_\parallel + B_z\gamma_e - \Delta_Z} \\
&+ \frac{B_\perp^2\gamma_e^2}{2 - A_\parallel - B_z\gamma_e - \Delta_Z} \\
E_{0,0} =& \frac{2A_\perp^2(A_\parallel - \Delta_Q - \Delta_Z)}{(A_\parallel - \Delta_Q - \Delta_Z)^2 - B_z^2(\gamma_e - \gamma_n)^2} + \frac{B_\perp^2\gamma_n^2}{2 - B_z\gamma_n - \Delta_Q} + \frac{B_\perp^2\gamma_n^2}{2B_z\gamma_n - \Delta_Q} \\
&+ \frac{B_\perp^2\gamma_e^2}{2 - B_z\gamma_e - \Delta_Z} + \frac{B_\perp^2\gamma_e^2}{2B_z\gamma_e - \Delta_Z} \\
E_{0,-1} =& \frac{A_\perp^2}{B_z\gamma_e - B_z\gamma_n + \Delta_Q - \Delta_Z} - B_z\gamma_n + \Delta_Q + \frac{B_\perp^2\gamma_n^2}{2\Delta_Q - B_z\gamma_n} + \frac{B_\perp^2\gamma_e^2}{2 - A_\parallel + B_z\gamma_e - \Delta_Z} \\
&+ \frac{B_\perp^2\gamma_e^2}{2A_\parallel - B_z\gamma_e - \Delta_Z} \\
E_{-1,+1} =& \frac{A_\perp^2}{-A_\parallel - B_z\gamma_e + B_z\gamma_n + \Delta_Q + \Delta_Z} + \frac{\epsilon_\perp^2}{-2A_\parallel - 2B_z\gamma_e} - A_\parallel - B_z\gamma_e + B_z\gamma_n + \Delta_Q + \Delta_Z \\
&+ \frac{B_\perp^2\gamma_n^2}{2 - A_\parallel + B_z\gamma_n + \Delta_Q} + \frac{B_\perp^2\gamma_e^2}{2 - A_\parallel - B_z\gamma_e + \Delta_Z} \\
E_{-1,0} =& \frac{A_\perp^2}{-B_z\gamma_e + B_z\gamma_n - \Delta_Q + \Delta_Z} - B_z\gamma_e + \Delta_Z - \frac{\epsilon_\perp^2}{2B_z\gamma_e} + \frac{B_\perp^2\gamma_n^2}{2 - A_\parallel + B_z\gamma_n - \Delta_Q} \\
&+ \frac{B_\perp^2\gamma_n^2}{2A_\parallel - B_z\gamma_n - \Delta_Q} + \frac{B_\perp^2\gamma_e^2}{2\Delta_Z - B_z\gamma_e} \\
E_{-1,-1} =& \frac{B_\perp^2\gamma_e^2}{2A_\parallel - B_z\gamma_e + \Delta_Z} - B_z\gamma_e + \frac{\epsilon_\perp^2}{2A_\parallel - 2B_z\gamma_e} + A_\parallel - B_z\gamma_n + \Delta_Q + \Delta_Z \\
&+ \frac{B_\perp^2\gamma_n^2}{2A_\parallel - B_z\gamma_n + \Delta_Q}
\end{aligned}$$

E Differences of Eigenvalues Hamiltonian

E.1 Measurable energies electron spin transitions

$$
\begin{aligned}
\omega_{e+}^{+1} =& \Delta_Z + A_\parallel + B_z\gamma_e + \frac{A_\perp^2}{B_z(\gamma_e-\gamma_n)-\Delta_Q+\Delta_Z} + \frac{\epsilon_\perp^2}{2A_\parallel+2B_z\gamma_e} - \frac{B_\perp^2\gamma_e^2}{2(A_\parallel+B_z\gamma_e-\Delta_Z)} \\
&+ \frac{B_\perp^2\gamma_e^2}{A_\parallel+B_z\gamma_e+\Delta_Z} + \frac{B_\perp^2\gamma_n^2}{2(A_\parallel+B_z\gamma_n+\Delta_Q)} - \frac{B_\perp^2\gamma_n^2}{2(B_z\gamma_n+\Delta_Q)} \\
\omega_{e-}^{+1} =& - \frac{A_\perp^2}{-B_z\gamma_e+B_z\gamma_n+\Delta_Q-\Delta_Z} + \frac{A_\perp^2}{-A_\parallel-B_z\gamma_e+B_z\gamma_n+\Delta_Q+\Delta_Z} + \frac{\epsilon_\perp^2}{-2A_\parallel-2B_z\gamma_e} \\
&- \frac{B_\perp^2\gamma_e^2}{2(A_\parallel+B_z\gamma_e-\Delta_Z)} - \frac{B_\perp^2\gamma_e^2}{2(-A_\parallel-B_z\gamma_e-\Delta_Z)} + \frac{B_\perp^2\gamma_e^2}{2(-A_\parallel-B_z\gamma_e+\Delta_Z)} \\
&+ \frac{B_\perp^2\gamma_n^2}{2(-A_\parallel+B_z\gamma_n+\Delta_Q)} - A_\parallel - B_z\gamma_e - \frac{B_\perp^2\gamma_n^2}{2(B_z\gamma_n+\Delta_Q)} + \Delta_Z \\
\omega_{e+}^{0} =& - \frac{2A_\perp^2(A_\parallel-\Delta_Q-\Delta_Z)}{(A_\parallel-\Delta_Q-\Delta_Z)^2-B_z^2(\gamma_e-\gamma_n)^2} + \frac{A_\perp^2}{B_z\gamma_e-B_z\gamma_n-\Delta_Q+\Delta_Z} \\
&- \frac{B_\perp^2\gamma_n^2\Delta_Q}{\Delta_Q^2-(A_\parallel+B_z\gamma_n)^2} + \frac{\epsilon_\perp^2}{2B_z\gamma_e} - \frac{B_\perp^2\gamma_e^2}{2(B_z\gamma_e-\Delta_Z)} + \frac{B_\perp^2\gamma_e^2}{B_z\gamma_e+\Delta_Z} \\
&+ B_z\gamma_e + \frac{B_\perp^2\gamma_n^2\Delta_Q}{\Delta_Q^2-B_z^2\gamma_n^2} + \Delta_Z \\
\omega_{e-}^{0} =& - \frac{2A_\perp^2(A_\parallel-\Delta_Q-\Delta_Z)}{(A_\parallel-\Delta_Q-\Delta_Z)^2-B_z^2(\gamma_e-\gamma_n)^2} + \frac{A_\perp^2}{-B_z\gamma_e+B_z\gamma_n-\Delta_Q+\Delta_Z} \\
&- \frac{B_\perp^2\gamma_n^2\Delta_Q}{\Delta_Q^2-(A_\parallel-B_z\gamma_n)^2} - \frac{\epsilon_\perp^2}{2B_z\gamma_e} - \frac{B_\perp^2\gamma_e^2}{2(-B_z\gamma_e-\Delta_Z)} \\
&- \frac{B_\perp^2\gamma_e^2}{B_z\gamma_e-\Delta_Z} - B_z\gamma_e - \frac{B_\perp^2\gamma_n^2}{2(-B_z\gamma_n-\Delta_Q)} - \frac{B_\perp^2\gamma_n^2}{2(B_z\gamma_n-\Delta_Q)} + \Delta_Z \\
\omega_{e+}^{-1} =& - \frac{A_\perp^2}{B_z\gamma_e-B_z\gamma_n+\Delta_Q-\Delta_Z} + \frac{A_\perp^2}{-A_\parallel+B_z\gamma_e-B_z\gamma_n+\Delta_Q+\Delta_Z} + \frac{\epsilon_\perp^2}{2B_z\gamma_e-2A_\parallel} \\
&- \frac{B_\perp^2\gamma_e^2}{2(-A_\parallel+B_z\gamma_e-\Delta_Z)} - \frac{B_\perp^2\gamma_e^2}{2(A_\parallel-B_z\gamma_e-\Delta_Z)} + \frac{B_\perp^2\gamma_e^2}{2(-A_\parallel+B_z\gamma_e+\Delta_Z)} \\
&+ \frac{B_\perp^2\gamma_n^2}{2(-A_\parallel-B_z\gamma_n+\Delta_Q)} + A_\parallel + B_z\gamma_e - \frac{B_\perp^2\gamma_n^2}{2(\Delta_Q-B_z\gamma_n)} + \Delta_Z \\
\omega_{e-}^{-1} =& - \frac{A_\perp^2}{B_z\gamma_e-B_z\gamma_n+\Delta_Q-\Delta_Z} + \frac{\epsilon_\perp^2}{2A_\parallel-2B_z\gamma_e} \\
&- \frac{B_\perp^2\gamma_e^2}{2(-A_\parallel+B_z\gamma_e-\Delta_Z)} - \frac{B_\perp^2\gamma_e^2}{2(A_\parallel-B_z\gamma_e-\Delta_Z)} + \frac{B_\perp^2\gamma_e^2}{2(A_\parallel-B_z\gamma_e+\Delta_Z)} \\
&+ \frac{B_\perp^2\gamma_n^2}{2(A_\parallel-B_z\gamma_n+\Delta_Q)} + A_\parallel - B_z\gamma_e - \frac{B_\perp^2\gamma_n^2}{2(\Delta_Q-B_z\gamma_n)} + \Delta_Z
\end{aligned}
$$

E.2 nitrogen spin transitions

$$
\begin{aligned}
\omega_{n+}^{+1} =& -\frac{A_\perp^2}{B_z\gamma_e - B_z\gamma_n - \Delta_Q + \Delta_Z} + \frac{\epsilon_\perp^2}{2A_\parallel + 2B_z\gamma_e} + \frac{B_\perp^2\gamma_e^2}{2(A_\parallel + B_z\gamma_e + \Delta_Z)} - \frac{B_\perp^2\gamma_n^2}{2(A_\parallel + B_z\gamma_n - \Delta_Q)} \\
& - \frac{B_\perp^2\gamma_n^2}{2(-A_\parallel - B_z\gamma_n - \Delta_Q)} + \frac{B_\perp^2\gamma_n^2}{2(A_\parallel + B_z\gamma_n + \Delta_Q)} + A_\parallel - \frac{\epsilon_\perp^2}{2B_z\gamma_e} - \frac{B_\perp^2\gamma_e^2}{2(B_z\gamma_e + \Delta_Z)} + B_z\gamma_n + \Delta_Q \\
\omega_{n-}^{+1} =& -\frac{A_\perp^2}{B_z\gamma_e - B_z\gamma_n - \Delta_Q + \Delta_Z} + \frac{A_\perp^2}{-A_\parallel + B_z\gamma_e - B_z\gamma_n + \Delta_Q + \Delta_Z} + \frac{\epsilon_\perp^2}{2B_z\gamma_e - 2A_\parallel} \\
& + \frac{B_\perp^2\gamma_e^2}{2(-A_\parallel + B_z\gamma_e + \Delta_Z)} - \frac{B_\perp^2\gamma_n^2}{2(A_\parallel + B_z\gamma_n - \Delta_Q)} - \frac{B_\perp^2\gamma_n^2}{2(-A_\parallel - B_z\gamma_n - \Delta_Q)} \\
& + \frac{B_\perp^2\gamma_n^2}{2(-A_\parallel - B_z\gamma_n + \Delta_Q)} - A_\parallel - \frac{\epsilon_\perp^2}{2B_z\gamma_e} - \frac{B_\perp^2\gamma_e^2}{2(B_z\gamma_e + \Delta_Z)} - B_z\gamma_n + \Delta_Q \\
\omega_{n+}^{0} =& -\frac{A_\perp^2}{A_\parallel - B_z\gamma_e + B_z\gamma_n - \Delta_Q - \Delta_Z} - \frac{A_\perp^2}{A_\parallel + B_z\gamma_e - B_z\gamma_n - \Delta_Q - \Delta_Z} + \frac{A_\perp^2}{-B_z\gamma_e + B_z\gamma_n + \Delta_Q - \Delta_Z} \\
& + \frac{B_\perp^2\gamma_e^2}{2(A_\parallel + B_z\gamma_e - \Delta_Z)} + \frac{B_\perp^2\gamma_e^2}{2(-A_\parallel - B_z\gamma_e - \Delta_Z)} - \frac{B_\perp^2\gamma_e^2}{2(-B_z\gamma_e - \Delta_Z)} - \frac{B_\perp^2\gamma_e^2}{2(B_z\gamma_e - \Delta_Z)} \\
& - \frac{B_\perp^2\gamma_n^2}{2(-B_z\gamma_n - \Delta_Q)} - \frac{B_\perp^2\gamma_n^2}{2(B_z\gamma_n - \Delta_Q)} + \frac{B_\perp^2\gamma_n^2}{2(B_z\gamma_n + \Delta_Q)} + B_z\gamma_n + \Delta_Q \\
\omega_{n-}^{0} =& -\frac{A_\perp^2}{A_\parallel - B_z\gamma_e + B_z\gamma_n - \Delta_Q - \Delta_Z} - \frac{A_\perp^2}{A_\parallel + B_z\gamma_e - B_z\gamma_n - \Delta_Q - \Delta_Z} + \frac{A_\perp^2}{B_z\gamma_e - B_z\gamma_n + \Delta_Q - \Delta_Z} \\
& + \frac{B_\perp^2\gamma_e^2}{2(-A_\parallel + B_z\gamma_e - \Delta_Z)} + \frac{B_\perp^2\gamma_e^2}{2(A_\parallel - B_z\gamma_e - \Delta_Z)} - \frac{B_\perp^2\gamma_e^2}{2(-B_z\gamma_e - \Delta_Z)} - \frac{B_\perp^2\gamma_e^2}{2(B_z\gamma_e - \Delta_Z)} \\
& - \frac{B_\perp^2\gamma_n^2}{2(-B_z\gamma_n - \Delta_Q)} - \frac{B_\perp^2\gamma_n^2}{2(B_z\gamma_n - \Delta_Q)} + \frac{B_\perp^2\gamma_n^2}{2(\Delta_Q - B_z\gamma_n)} - B_z\gamma_n + \Delta_Q \\
\omega_{n+}^{-1} =& -\frac{A_\perp^2}{-B_z\gamma_e + B_z\gamma_n - \Delta_Q + \Delta_Z} + \frac{A_\perp^2}{-A_\parallel - B_z\gamma_e + B_z\gamma_n + \Delta_Q + \Delta_Z} + \frac{\epsilon_\perp^2}{-2A_\parallel - 2B_z\gamma_e} \\
& + \frac{B_\perp^2\gamma_e^2}{2(-A_\parallel - B_z\gamma_e + \Delta_Z)} - \frac{B_\perp^2\gamma_n^2}{2(-A_\parallel + B_z\gamma_n - \Delta_Q)} - \frac{B_\perp^2\gamma_n^2}{2(A_\parallel - B_z\gamma_n - \Delta_Q)} \\
& + \frac{B_\perp^2\gamma_n^2}{2(-A_\parallel + B_z\gamma_n + \Delta_Q)} - A_\parallel + \frac{\epsilon_\perp^2}{2B_z\gamma_e} - \frac{B_\perp^2\gamma_e^2}{2(-B_z\gamma_e + \Delta_Z)} + B_z\gamma_n + \Delta_Q \\
\omega_{n-}^{-1} =& -\frac{A_\perp^2}{-B_z\gamma_e + B_z\gamma_n - \Delta_Q + \Delta_Z} + \frac{\epsilon_\perp^2}{2A_\parallel - 2B_z\gamma_e} + \frac{B_\perp^2\gamma_e^2}{2(A_\parallel - B_z\gamma_e + \Delta_Z)} \\
& - \frac{B_\perp^2\gamma_n^2}{2(-A_\parallel + B_z\gamma_n - \Delta_Q)} - \frac{B_\perp^2\gamma_n^2}{2(A_\parallel - B_z\gamma_n - \Delta_Q)} + \frac{B_\perp^2\gamma_n^2}{2(A_\parallel - B_z\gamma_n + \Delta_Q)} + A_\parallel \\
& + \frac{\epsilon_\perp^2}{2B_z\gamma_e} - \frac{B_\perp^2\gamma_e^2}{2(-B_z\gamma_e + \Delta_Z)} - B_z\gamma_n + \Delta_Q
\end{aligned}
$$

References

[1] Quantum Vision Team. *Quantum Internet.* Magazine (June 2019).

[2] Cramer, J. (2016) *Quantum error correction with spins in diamond.* (PhD Thesis). TU Delft, Delft.

[3] Franz Rellich and J. Berkowitz. *Perturbation Theory of Eigenvalue Problems,* pages 29-37. Gordon and Breach, (1969)

[4] Griffiths, David J. *Introduction to Quantum Mechanics Second Edition.* Cambridge University Press, Cambridge (2017).

[5] M. H. Abobeih, J. Randall, C. E. Bradley, H. P. Bartling, M. A. Bakker, M. J. Degen, M. Markham, D. J. Twitchen, T. H. Taminiau. *Atomic-scale imaging of a 27-nuclear-spin cluster using a single-spin quantum sensor.* arXiv:1905.02095 [quant-ph] (2019).

[6] Toeno van der Sar, Francesco Casola, Ronald Walsworth, Amir Yacoby. *Nanometre-scale probing of spin waves using single electron spins.* Nature Communications volume 6, Article number: 7886 (2015)

[7] Marcus W. Doherty, Neil B. Manson, Paul Delaney, Fedor Jelezko, Jörg Wrachtrup, and Lloyd C. L. Hollenberg. The nitrogen-vacancy colour center in diamond. *Physics Reports*, 528(1):1–45, 2013.

[8] *https://www.chemistryworld.com/news/putting-a-new-spin-on-things/3007939.article*

[9] M. H. Abobeih, J. Cramer, M. A. Bakker, N. Kalb, M., Markham, D. J. Twitchen, T. H.Taminiau *One-second coherence for a single electron spin coupled to a multi-qubit nuclear-spin environment.* Nature Communications volume 9, Article number: 2552 (2018)

[10] M A Bernstein; K F King; X J Zhou (2004). *Handbook of MRI Pulse Sequences.* San Diego: Elsevier Academic Press. p. 960. ISBN 0-12-092861-2.